DOKUZ EYLÜL UNIVERSITY
GRADUATE SCHOOL OF NATURAL AND APPLIED SCIENCES

FUZZY TECHNIQUES IN IMAGE PROCESSING FOR RISK ASSESSMENT OF SKIN DISEASES

by
İsmail CANOĞLU

July, 2021
İZMİR

FUZZY TECHNIQUES IN IMAGE PROCESSING FOR RISK ASSESSMENT OF SKIN DISEASES

A Thesis Submitted to the
Graduate School of Natural And Applied Sciences of Dokuz Eylül University
In Partial Fulfillment of the Requirements for the Degree of Master of Science in Computer Science

by
İsmail CANOĞLU

July, 2021
İZMİR

M.Sc THESIS EXAMINATION RESULT FORM

We have read the thesis entitled "**FUZZY TECHNIQUES IN IMAGE PROCESSING FOR RISK ASSESSMENT OF SKIN DISEASES**" completed by **İSMAİL CANOĞLU** under supervision of **PROF. DR. EMEL KURUOĞLU KANDEMİR** and we certify that in our opinion it is fully adequate, in scope and in quality, as a thesis for the degree of Master of Science.

.....

Prof. Dr. Emel KURUOĞLU KANDEMİR

Supervisor

.....	.....
Prof. Dr. Çağın KANDEMİR ÇAVAŞ	Prof. Dr. Urfat NURİYEV
Jury Member	Jury Member

Prof. Dr. Özgür ÖZÇELİK
Director
Graduate School of Natural and Applied Sciences

ACKNOWLEDGEMENTS

Firstly, I would like to express my sincere gratitude to my supervisor Prof. Dr. Emel KURUOĞLU KANDEMİR for the guidance she has shown throughout this study, belief in me have led to the completion of this study. I also would like to thank Prof. Dr. Vildan MEVSİM for her medical support.

Although I have a slightly narcissistic attitude, I want to thank myself first. I leave my patience, effort, dreams, hopes and more on these pages as a trace as I always do. The nights that I didn't sleep at the beginning of the thesis, my looking at the screen without writing a word, all blend into a good memory. When I look back, a smile will appear on my face.

Lastly, I am very grateful to my family for their trust and endless love, which is the greatest support in my life.

İsmail CANOĞLU

FUZZY TECHNIQUES IN IMAGE PROCESSING FOR RISK ASSESSMENT OF SKIN DISEASES

ABSTRACT

Many skin diseases are now documented in the literature. There may be some difficulties in diagnosing them while it is simple to observe them. Mole is a pigmented spot or small permanent protuberance on the human body that can be divided into malignant and benign categories. Melanoma is the medical term for a malignant mole. Melanoma-induced skin cancer is one of these observable diseases. Early diagnosis is critical for this cancer, which is relatively easy to treat once discovered. But disease diagnosis is a difficult stage in medicine. Diagnosis is based on a patient's signs, symptoms, physical examination, and some tests. However, a single human experience or opportunities may not be enough for the correct diagnosis. Such situations cause problems when doctors make the diagnosis. Developing computer technologies and machine learning techniques are applied to systems that will help doctors in the early diagnosis of diseases. In this study, a decision support system is studied for the detection of melanoma.

Keywords: Melanoma, ANFIS, fuzzy logic, decision support system, artificial neural network

DERİ HASTALIKLARININ RİSK DEĞERLENDİRMESİ İÇİN GÖRÜNTÜ İŞLEMEDE BULANIK TEKNİKLER

ÖZ

Günümüzde literatürde tanımlı birçok deri hastalığı vardır. Onları gözlemlemek çok kolay olsa da tanıda bazı problemler olabilir. İnsan vücudunda pigmentli bir nokta, işaret veya küçük kalıcı bir çıkıntı olarak tanımlanan ben, basitçe iyi huylu ve kötü huylu ayrılabilir. Malign bene Melanom adı verilir. Bu gözlemlenebilir hastalıklardan biri, melanomun neden olduğu cilt kanseridir. Erken tanı bu kanser için çok önemlidir, bu tanı konulduğunda tedavi edilmesi kolaydır. Ama hastalık teşhisi tıpta zor bir aşamadır. Teşhiste bir hastanın bulgu, semptom, fizik muayenesi ve bazı testlere dayanır. Ancak doğru tanı için tek bir insan tecrübesi ya da imkanlar yeterli olmayabilir. Bu gibi durumlar doktorların teşhisi koyarken sorunlara sebep olmaktadır. Gelişen bilgisayar teknolojileri ve makine öğrenme teknikleri hastalıkların erken teşhisinde doktorlara yardımcı olacak sistemlere uygulanmaktadır. Bu çalışmada, melanomun tespiti için karar destek sistemi üzerinde çalışılmıştır.

Anahtar kelimeler: Melanom, ANFIS, bulanık mantık, karar destek sistemi, yapay sinir ağı

CONTENTS

Page

LIST OF FIGURES

Page

LIST OF TABLES

Page

CHAPTER ONE
INTRODUCTION

Cancer is too old to be among the diseases of the modern age. Tumours in fossilized bones and mummies found in Egypt provide evidence of cancer cases. As far as is known, there are findings about breast cancer in ancient medical manuscripts written around 3000 BC (José Costa, 2020). They even said that "**There is no treatment**" for cancer.

The modern age and developing technology have provided us with great opportunities in diagnosis and treatment. Especially the technological advances in the last century, the invention of the computer and the progress in medical imaging systems make some processes easier. Therefore, we human beings should take advantage of this in order to relieve pain and make life a better place. This study is an idea put forward in order to serve it. Between 2011 and 2017, the 5-year Relative Survival rate was found to be 93.3% (The Surveillance, Epidemiology, and End Results, 2021). Skin cancer, based melanoma, is a kind of cancer with a high 5-year survival rate, as seen in the Table 1.1 (The Surveillance, Epidemiology, and End Results, 2021). The treatment of melanoma varies according to the stage at which it is diagnosed. Increase in the size of melanoma and progressive stages increase the risk of metastasis (Grossniklaus, 2013).

Table 1.1 New cases/deaths per 100,000 & 5_years survival percentages

	New Cases Rate [a]		New Cases Rate [b]		Death Rate — U.S.		5-Year Relative Survival [a]	
Year	Observation	Modeled Trend	Observation	Modeled Trend	Observation	Modeled Trend	Observation	Modeled Trend
2010	23.96	23.37	21.48	21.07	2.74	2.70	93.96%	94.35%
2011	23.01	23.70	20.55	21.43	2.69	2.69	93.97%	94.55%
2012	23.10	24.03	20.86	21.80	2.66	2.69	95.20%	94.74%
2013	24.25	24.37	21.83	22.18	2.67	2.69	95.81%	94.93%
2014	25.48	24.72	23.02	22.56	2.57	2.54	-	95.11%
2015	25.93	25.07	23.21	22.95	2.41	2.40	-	95.28%
2016	25.79	25.42	23.11	23.34	2.17	2.26	-	95.45%
2017	25.62	25.78	22.80	22.84	2.09	2.13	-	95.61%
2018	25.32	26.14	22.37	22.35	2.08	2.01	-	95.77%

[a] SEER 9, [b] SEER 13.

Global climate change, the ozone depletion and genetic selection are probably

effective in the increase of melanoma related skin cancer. The data in the Table 1.1 allows us to say this. Something is changing in our world. We have to do something to compensate for the damage we have done to the world. Returning to our topic, many scientists have studied melanoma for years. Let's take a look at the works done about melanoma at this stage.

The colour is important factor to detect melanoma. Because melanoma includes blue, dark brown, black, tan, red and, sometimes grey or a mixture of those colours. So capturing these colours leads to new research about this area. One of them belongs to Colot et al. (1998). They used the dataset includes 38 lesions (20 bening and 18 malignant). Preprocess, segmentation and classification are done, respectively. They tried to describe of the colour and the shape of the lesions.

Chung & Sapiro (2000) used partial differential equations for boundary detection. The image was preprocessed by changing concentration and anisotropic diffusion. Then boundaries are detected by using geodesic active contours model. In this work, we can see multidisciplinary work among mathematics and computer science.

In the work of Ganster et al. (2001), skin lesion is obtained as binary form by using some segmentation algorithms. A group of features set, which includes shape and radiometric features, are worked on for determining the melanoma. After selected features, last k-NN gives high sensitivity (87%) with high specificity (92%).

Schmid-Saugeona et al. (2003) work is focused on symmetry, especially. Firstly, the lesion boundary is detected. Then degree of symmetry is calculated. Working data were validated by specialist doctors. In this way, it is calculated the accuracy of boundary, that obtained by computer-aided system, statistically. For classification of skin lesion as bening or malignant, six dimensional feature vector is used providing the symmetry quantification. This research shows that outperforms principal component decomposition approaches.

Rajab et al. (2004) tries to solve skin image segmentation problem by two ways. One of them is region segmentation which is determined by an isodata algorithm which

data is organizing itself, iteratively. The other one is fitting of edge detected by neural network and Gaussian curve, so closed elastic curve is obtained around neural network edge patterns, approximately.

90 dermoscopy images are used by Emre Celebi et al. (2008). The borders are determined by algorithm based on statistical region merging. That algorithm is compared with 4 automated methods. As a result, algorithm works fast and accurate than other methods.

In Ruiz et al. (2011) work ,decision support system is designed. The system work comparing some classification methods like a Bayesian classifier, a multilayered perceptron and the algorithm of the K nearest neighbours. The result is obtained by comparing the methods calculated separately. The classification success is around 87%.

289 dermoscopy images (114 malignant, 175 benign) is used by Garnavi et al. (2012) as three group: test, validation and train. The classification was made using 4 methods (Support Vector Machine, Random Forest, Hidden Naive Bayes, and Logistic Model Tree) and 23 features. 23 features are selected using wavelet for texture, boundary-series for border and shape indexes for geometry. The system works with high accuracy (91.26%) and high AUC value (0.937).

Importance of noise removing is the main topic of work of Hoshyar et al. (2014). So the performance of the 5 filters has been compared. The compared noise filters are as follows: Mean Filter, Median Filter, Adaptive Wiener filter, Adaptive Median Filter, and Gaussian Filter.

In the first stage, a mask is created with machine learning within some rules. Then, a structure analysis is made through this mask, and the pigment network is tried to be determined. If available, the mask corresponding to this model is created. Arroyo & Zapirain (2014), who performed the test with 220 photos, achieved 86% sensitivity and 81.67% specificity.

Skin images are filtered and segmented. Texture and colour features are gotten from lesions. They are classified by two classification methods like SVM and k-NN. Sumithra et al. (2015) tested the system for 5 diseases, 141 images and 726 samples. Measure of F using k-NN and SVM get 46.71% and 34% respectively and it is measured 61% of measure of F for k-NN and SVM.

In Jain et al. (2015) work, lesions are classified benign and Melanoma based lesion of cancer. The parameters as ABCD are used for classification.

Almubarak et al. (2017) demonstrated fuzzy based colour histogram analysis. Support set cardinality and alpha-cut to quantify a fuzzy ratio colour feature of skin lesion is used. 517 dermoscopy images (175 melanomas, 342 benigns) are clustered using the fuzzy clustering. Fuzzy clustering is a 8-neighborhood on the outer 25% of the skin lesion alpha-cut level 0.08. It is determined melanomas correctness 92.6% with 13.5% false positive lesions.

The part of the story about me is all about immortality. Science may not have discovered immortality yet, but leaving something permanent will pave the way for immortality. there is much to be done to become one of the stars in the sky and this work is the very beginning of the road. In this context, we started this thesis. First, we focused on fuzzy logic to use in the study. then we had to make sense of melanoma. For this, we benefited from the dermatology literature. Basic knowledge of the skin was necessary to understand what melanoma is. The skin was learned with the necessary researches and inquiries. The data to be used in the study should have been obtained from images. This necessitated learning image processing. Image processing was focused on to obtain the input values to be used in the model. The method chosen for the model is artificial neural network. The artificial neural network has been studied at the required level. Finally, this information was blended and the model design was completed.

It aims to get rid of this disease as soon as possible by creating a decision support system for the early diagnosis of melanoma-related skin cancer. In this direction, the

designed decision support system works in 3 steps. Processing the image of the lesion, applying the data obtained from the processed image to the model and interpreting the outputs. This will facilitate diagnosis.

CHAPTER TWO
CONCEPT: LOGIC

Opinions on logic have been going on since the existence of mankind. These views have evolved over time into some formalized languages, including the concept of well-formed formulas. The simplest form is existence and non-existence. The binary version is defined as 0 and 1. These describe as the existence and its opposite situation like Shakespeare (1912) said in Hamlet "To be, or not to be, that is the question". And the whole system is built on it. But mathematicians have been driven into the search for a system beyond the binary system with the curiosity motive given by mathematics. This quest has contributed to the discovery of multi-valued logic theories. Bochvar's "interval" and "external" system, Łukasiewicz logics, Gödel logics and Post logics have the most accepted theories in the field of multi-valued logic. Let's examine the journey from logic to multi valued logic and from there to fuzzy logic.

2.1 Aristotle's Logic

Mathematics and logic became an inseparable whole in modern times, although they emerged as different disciplines in the historical order. Over time, mathematics has become more logical and logic more mathematical. Classical logic reveals certain situations with binary value system. Sets are defined as a collection or group that created by objects or elements (provided that they are different and well-defined). The objects of a set are called the elements of that set, that is, the objects belong to the set. If the objects do not belong to the set, they are not members of the set. Classical sets are expressed in definite, clear and undoubted limitations. Let set E be a universal set, and set A be a subset of the universal set E, $A \subset E$. Suppose that there are two elements a_1 and a_2. a_1 belongs to the set A and a_2 does not belong to set A. They are expressed as $a_1 \in A$ and $a_2 \notin A$, respectively$(a_1 \wedge a_2 \in E)$.

2.2 Bochvar's Logic

In Bochvar (1939) there are two different logic systems, called the "internal" and "external" systems. In the internal system, the number of different intermediate output values is limited to a single intermediate value, so that the only other output values are F and T. In the external system this single intermediate entry is resolved to either F or T so that there are no intermediate output values in the resulting table (Epstein, 1993). These logics were illustrated for conjunction using the categorical tables in Table 2.1 and Table 2.2.

Table 2.1 Bochvar's interval conjunction

	F	E_1	E_2	E_3	T
F	$\boldsymbol{F}$	E_2	E_2	E_2	$\boldsymbol{F}$
E_1	E_2	E_2	E_2	E_2	E_2
E_2	E_2	E_2	E_2	E_2	E_2
E_3	E_2	E_2	E_2	E_2	E_2
T	$\boldsymbol{F}$	E_2	E_2	E_2	$\boldsymbol{T}$

Table 2.2 Bochvar's external conjunction

	F	E_1	E_2	E_3	T
F	$\boldsymbol{F}$	T	T	T	$\boldsymbol{F}$
E_1	F	F	F	F	F
E_2	F	F	F	F	F
E_3	F	F	F	F	F
T	$\boldsymbol{F}$	F	F	F	$\boldsymbol{T}$

2.3 Łukasiewicz Logics

For Łukasiewicz, propositional functions' logical values were a starting point for further thoughts. Propositional functions include a precisely defined field including finite individuals. A propositional function's logical value is determined by the ratio of the number of elements that satisfy it to the cardinality of the entire domain. If it is satisfied by no element, a propositional function is called false; in the other case, it is true. Hence, it takes 0 or 1. It follows that propositional functions with values δ except 0 and 1 are existed, and that they must have $0 < \delta < 1$. The probability of $\alpha(x)$ is then δ. The logical value of α is referred to as δ (Bolc & Borowik, 2013a).

Let α, β be any propositional functions and let $w(\alpha)$, $w(\beta)$ denote their logical values. The symbols $\sim\alpha$ and $\alpha \vee \beta$, $\alpha \wedge \beta$, $\alpha \iff \beta$, $\alpha \Rightarrow \beta$ show the negation of α and the disjunction, conjunction, equivalence, α implicates to β, respectively. He accepts the following axioms for own probability calculus (α, β refer for propositional):

(a_1) if α is true then $w(\alpha) = 1$;

(a_2) if α is false then $w(\alpha) = 0$;

(a_3) if $w(\alpha \Rightarrow \beta) = 1$ then $w(\sim\alpha + \beta) + w(\alpha) = w(\beta)$.

The axioms also have the following features, which hold for any propositional functions $alpha, beta$:

(b_1)

$$\text{if } w(\alpha \iff \beta) = 1 \text{ then } w(\alpha) = w(\beta); \tag{2.1}$$

(b_2)

$$w(a) + w(\sim a) = 1; \tag{2.2}$$

(b_3)

$$w(\sim a \wedge \beta) + w(\alpha \wedge \beta) = w(\beta); \tag{2.3}$$

(b_4)

$$w(\sim a \wedge \beta) + w(\alpha) = w(\alpha \vee \beta); \tag{2.4}$$

(b_5)

$$w(\alpha \vee \beta) = w(\alpha) - w(\alpha \wedge \beta) + w(\beta); \tag{2.5}$$

(b_6)

$$\text{if } w(\alpha \wedge \beta) = 0 \text{ then } w(\alpha \vee \beta) = w(\alpha) + w(\beta). \tag{2.6}$$

2.4 Gödel's Multivalued Logic Work

In a rough-and-ready fashion, Gödel logics is described as follows: The logics are multivalued, and the truth value sets considered are closed subsets of $[0, 1]$ that include both 0 and 1. If it yields the value 1 in entire interpretation, a formula is valid 1 is the "designated value". The conditional of Gödel , a distinctive Gödel logics operator, is described by $a \leftarrow b = 1$ if $a \leq b$ and $= b$ if $a > b$. Since the truth values are ordered, the semantics of Gödel logics is well suited to formalize comparisons. In this way, it's similar to Łukasiewicz (or "fuzzy") logic, a more noted multiple-valued logic, however just comparison does not define the Łukasiewicz conditional truth function. Gödel logics are logics of relative comparison, as opposed to Łukasiewicz idea, that may be termed a logic of metric or absolute comparison. This alone makes his logics works a fascinating topic for logical researches (Baaz, Preining & Zach, 2007).

2.5 Post Logics

Unlike Łukasiewicz, Post logics defines as finite-valued. Post had been inspired by the classical logic in *Principia Mathematica* by A.N. Whitehead and B. Russel (Karpenko, 2006). The main idea of Post was a generalization for a finite set of truth-values of the classical logic. The *n*-valued Post connectives are functions that act on a set of *n* items, which are seen as logical values. There are lots of functions

whose meaning in propositional calculus appears to be somewhat unnatural (Bolc & Borowik, 2013b).

(a)

$$J_k(x) = \begin{cases} 0 & \text{if } x \neq k, \\ n-1 & \text{if } x = k, \end{cases} \tag{2.7}$$

(b)

$$j_k(x) = \begin{cases} 1 & \text{if } x = k, \\ 0 & \text{if } x \neq k, \end{cases} \tag{2.8}$$

(c)

$$\min x, y = x \wedge y, \tag{2.9}$$

(d)

$$\max x, y = x \vee y, \tag{2.10}$$

(e)

$$(x - y) mod n, \tag{2.11}$$

(f)

$$(x + y) mod n. \tag{2.12}$$

Some negation properties are imitated by functions J_k for $k \neq n-1$. For all j_k is the characteristic function of its index k; furthermore, certain features of the idea of negation may be observed in the j_k's. Generalizations of disjunction and conjunction expressed in functions (e) and (f).

Any of the functions defined by (c), (d), (e), or (f) can be represented by $xcircy$. Then:

(a)

$$x \circ y = y \circ x, \tag{2.13}$$

(b)

$$x \circ (y \circ z) = (x \circ y) \circ z, \tag{2.14}$$

(c)

$$(x \wedge y) \vee z = (x \vee z) \wedge (y \vee z), \tag{2.15}$$

(d)

$$(x \vee y) \wedge z = (x \wedge z) \vee (y \wedge z), \tag{2.16}$$

(e)

$$J_k J_i(x) = J_k(J_i(x)) = \begin{cases} V_{\substack{s=0 \\ s \neq i}}^{n-1} & \text{if } k = 0, \\ 0 & \text{if } 0 < k < n-1, \\ J_i(x) & \text{if } k + n - 1, \end{cases} \tag{2.17}$$

(f)

$$J_k(x \vee y) = (J_k(x) \wedge V_{s=0}^{k} J_s(y)) \vee (J_k(y) \wedge V_{s=0}^{k} J_s(x)), \tag{2.18}$$

(g)

$$J_k(x \wedge y) = (J_k(x) \wedge V_{s=k}^{n-1} J_s(y)) \vee (J_k(y) \wedge V_{s=k}^{n-1} J_s(x)), \tag{2.19}$$

(h)

$$x = V_{i=0}^{n-1}(i \wedge j_i(x)) \tag{2.20}$$

(elimination of ”pure” occurences of a variable),

(i)

$$x = x \wedge V_{i=0}^{n-1} J_i(y) \tag{2.21}$$

(introduction of a variable)

(j) cancellation laws:

$$J_s(x)J_t(x) = \begin{cases} J_s(x) & \text{if } s = t, \\ 0 & \text{if } s \neq t, \end{cases} \tag{2.22}$$

$(n-1) \wedge x = x,$

$(n-1) \vee x = n-1,$

$0 \wedge x = 0,$

$0 \vee x = x,$

(k) each function $f : (\bar{n})^m \to \bar{n}$ can be indicated as

$$f(x_1, x_2, \ldots, x_m) = \bigvee_{\substack{(s_1,s_2,\ldots,s_m) \\ s_i \in \bar{n}}} (\bigwedge_{i=1}^{m} J_{s_i}(x_i) \wedge f(s_1, s_2, \ldots, s_m)), \tag{2.23}$$

named the disjunctive normal form of f.

2.6 Fuzzy Logic

Traditional tools for formal computing, modelling, and reasoning are deterministic, precise, and crisp. Crisp denotes dichotomous, i.e., no/yes type rather than less/more. All description of a real system many times requires much as well detailed data than a person can recognize, process and understand at the same time. This has long been acknowledged by philosophers. B. Russell, a philosopher, made his first argument in 1923: ”All conventional logic routinely presupposes the use of exact symbols. “As a result, it is only relevant to an imagined heavenly existence and not to our terrestrial one’’. Then, “As a system becomes more complicated, our capacity to make accurate and yet meaningful assertions about its behavior declines until a threshold is reached beyond which accuracy and importance (or relevance) become nearly mutually incompatible characteristics,” L. Zadeh said. The first publications in fuzzy set theory by Zadeh and Goguen demonstrate the authors’ intent to generalize the classical

notion of a set and a proposition to accommodate fuzziness in the sense that it is expressed in human language, i.e., in decisions, evaluation, and human judgment (Zimmermann, 2010).

Formally, for all fuzzy set A is a fuzzy subset of universal set U, expressed by membership function of A $\mu_A : u \rightarrow [0,1]$. The value $\mu_A(x)$ is the membership degree of x with respect to A that is the fuzzy set (Gottwald 2015; Zadeh 1965).

In classical logic, there is a distinction between the element of the set and the non-element of the set. The definition of belonging to the set A, which is a function representing α an object and $\mu(\alpha)$ degree of membership function of A, is expressed as mathematical logic as follows:

$$\mu_A(x) = \begin{cases} 1, & \text{if } a \in A \\ 0, & \text{if } a \notin A. \end{cases} \tag{2.24}$$

2.6.1 Fuzzy Logic Theory

The most important development point about Fuzzy Logic was expressed by Zadeh in 1965. In fact, years ago, mathematicians and philosophers laid the foundations for the subject of uncertainty. Zadeh's work is a milestone in this area. In his study, Zadeh defined the class of the degree of permanent membership of objects as a fuzzy set (Zadeh, 1965). Zadeh argued that the cluster has a membership function and the degree of membership that each object of the cluster has between 0 and 1. The adjectives such as long, medium, short, beautiful, ugly, hot and cold, which we use daily in our language, actually have degrees varying from person to person. For example, in the Figure 2.1 graph below (Jang, Sun & Mizutani, 1997), young, middle and old is defined by age ranges.

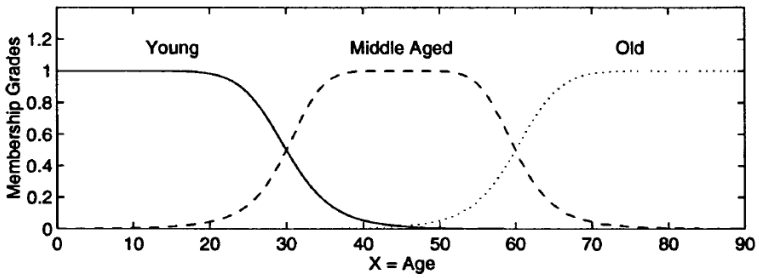

Figure 2.1 ”young,” ”middle,” and ”old” linguistic values

2.6.2 Fuzzy Sets

In fuzzy sets, boundaries are not clear, uncertainty exists. The boundaries are blurred, as they are expressed by indeterminate features and definitions. The membership function, $\mu_x(a)$, does not take precisely 0 or 1, as in conventional sets;$[0, 1]$ takes a value in the range. If the value of any member, membership function is close to 0, with a low degree to the set; If it is close to 1, it belongs to the cluster with a high degree.

The value of the degree of membership defined by Zadeh for fuzzy sets is in real, continuous, unit range $(\mu_A(x) \in [0, 1])$. If the value is 0 and 1, it means that there is no membership and a full membership, respectively. There are infinite values in the unit range, so there can be many membership degree values and definitions for an element in the universal set.

The definition of the fuzzy set A within the universal set E can be made as follows depending on the set E:

$$[h]A = \begin{cases} \int_E \mu_A(x)/x, & \text{If the universal set E is continuous,} \\ \sum_{x_1 \in E} \mu_A(x_i)/x_i, & \text{If E has a finite elements.} \end{cases} \tag{2.25}$$

Fuzzy membership functions are defined on discrete and continuous sets Figure 2.2 (Jang et al., 1997).

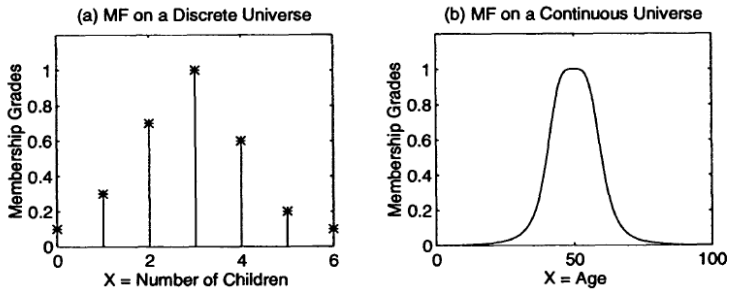

Figure 2.2 (a) A= ”children in a family”; (b) B = ”around 50 years old”

2.6.3 Terminology and Definitions

Definition 2.6.3.1. Membership Functions

A **fuzzy set** set A in X is defined as a set of ordered pairings if X is a collection of objects indicated generically by x.

$$A = \{(x, \mu_A(x))|x \in X\}, \tag{2.26}$$

in which $\mu_A(x)$ is named the **membership function** (or **MF**) for A. The maps of MF for all element of X to a membership value between 0 and 1 (Jang et al., 1997).

Definition 2.6.3.2. Support

The set of individual points in a fuzzy set A is called **support**. x in X, i.e. $\mu_A(x) > 0$:

$$support(A) = \{x|\mu_A(x) > 0\}. \tag{2.27}$$

Definition 2.6.3.3. Core

The set of individual points in a fuzzy set A is called the **core**. x in X implies $\mu_A(x) = 1$:

$$core(A) = \{x|\mu_A(x) = 1\}. \tag{2.28}$$

Definition 2.6.3.4. Normality

A fuzzy set A is **normal** if its core is nonempty. To put it another way, a point $x \in X$ can always be identified where $\mu_A(x) = 1$.

Definition 2.6.3.5. Crossover Points

A **crossover point** of a fuzzy set A is a point $x \in X$ where $\mu_A(x) = 0.5$:

$$crossover(A) = \{x|\mu_A(x) = 0.5\}. \tag{2.29}$$

Definition 2.6.3.6. Fuzzy Singleton

Fuzzy singleton is defined as support of fuzzy set equals a single point i.e. $\mu_A(x) = 1$.

The cores, supports, and crossover points of the bell-shaped membership function describing ”middle aged” and the fuzzy singleton characterizing ”45 years old” are depicted in Figure 2.3 (Jang et al., 1997).

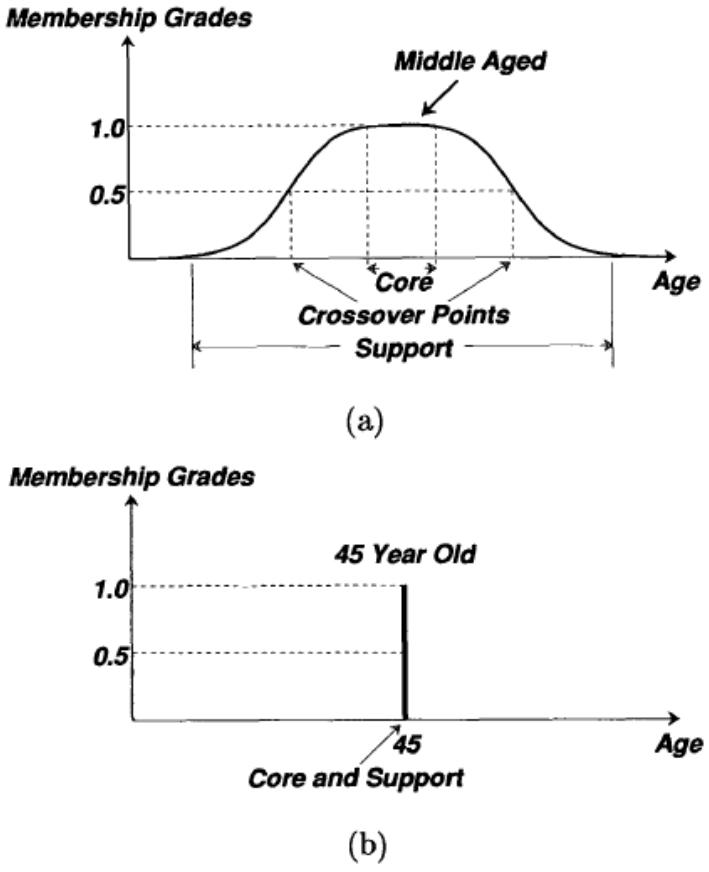

Figure 2.3 Crossover points, supports, and cores of (a)middle aged and (b)”45 years old” singleton

Definition 2.6.3.7. α-cut

The α**-cut** of a fuzzy set A is described by

$$A_\alpha = \{x|\mu_A(x) \geq \alpha\}. \tag{2.30}$$

Storng α**-cut** are described the same:

$$A'_\alpha = \{x|\mu_A(x) > \alpha\}. \tag{2.31}$$

The support and core of fuzzy set A may be represented using level set notation as follows:

$$support(A) = A'_0, \tag{2.32}$$

and

$$core(A) = A_1, \tag{2.33}$$

respectively.

Definition 2.6.3.8. Convexity

If and only if for each $x_1, x_2 \in X$ and any $\lambda \in [0, 1]$, a fuzzy set A is **convex**,

$$\mu_A(\lambda x_1 + (1 - \lambda)x_2) \geq min\{\mu_A(x_1), \mu_A(x_2)\}. \tag{2.34}$$

In an other saying, if entire α-level sets are convex, A is convex.

Figure 2.4 shows the concept of convexity.

Definition 2.6.3.9. Fuzzy numbers

A fuzzy number A defines as a fuzzy set on the real number $(\mathbb{R})$ that satisfies the convexity and normality conditions.

Definition 2.6.3.10. Bandwidth of convex and normal fuzzy sets

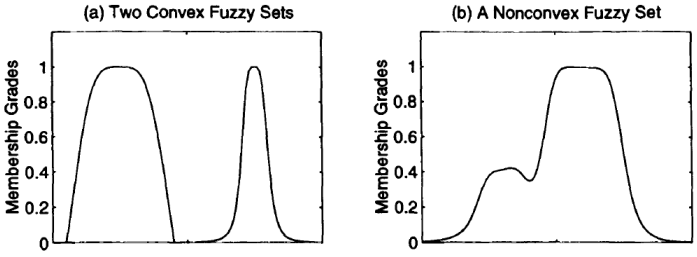

Figure 2.4 (a) 2 convex MF; (b) a nonconvex MF.

For a convex and normal fuzzy set, the **bandwidth** is described as the distance between the two unique crossover points:

$$width(A) = |x_2 - x_1|, \tag{2.35}$$

where $\mu_A(x_1) = \mu_A(x_2) = 0.5$.

Definition 2.6.3.11. Symmetry

If membership function is symmetric about a certain point $x = p$, a fuzzy set A is **symmetric** , namely,

$$\mu_A(p + x) = \mu_A(p - x) \text{ for all } x \in X. \tag{2.36}$$

Definition 2.6.3.12. Open left, open right, closed

If $\lim_{x\to-\infty} \mu_A(x) = 1$ and $\lim_{x\to+\infty} \mu_A(x) = 0$, it is called **open left**; if $\lim_{x\to-\infty} \mu_A(x) = 0$ and $\lim_{x\to+\infty} \mu_A(x) = 1$, it is called **open right** ; and if $\lim_{x\to+\infty} \mu_A(x) = \lim_{x\to+\infty} \mu_A(x) = 0$, it is called **closed**.

2.6.4 Set-Theoretic Operations

Fuzzy sets have operations that are analogous to the regular set operations of complement, union, and intersection, which were first described by Zadeh. Some essential ideas must first be developed in order to introduce these fuzzy set operations.

Definition 2.6.4.1. Containment or subset

If and only if $\mu_A(x) \leq \mu_B(x)$ for all x, fuzzy set A is **contained** in fuzzy set B (or, equivalently, A is a **subset** of B, or A is smaller than or equal to B). In terms of symbolism,

$$A \subseteq B \iff \mu_A(x) \leq \mu_B(x). \tag{2.37}$$

Figure 2.5 shows $A \subseteq B$.

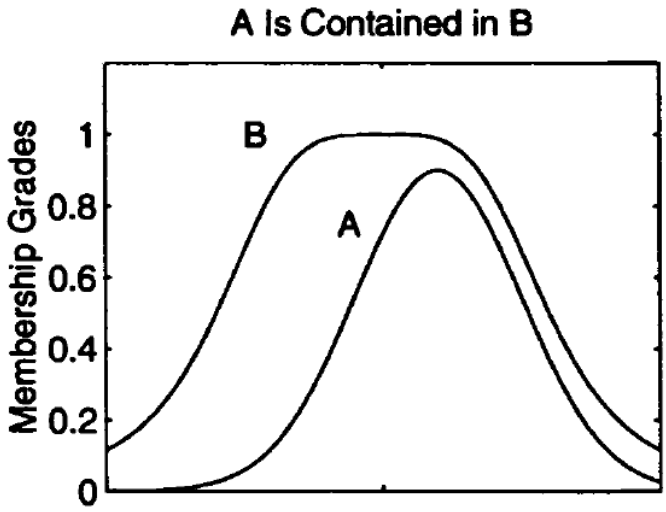

Figure 2.5 The concept of $A \subseteq B$.

Definition 2.6.4.2. Union (disjunction)

The **union** of two fuzzy sets A and B provides a fuzzy set C, which may be represented as $C = A \cup B$ or $C = A$ OR B, and its membership function is involved to those of A and B by

$$\mu_C(x) = max(\mu_A(x), \mu_B(x)) = \mu_A(x) \vee \mu_B(x). \tag{2.38}$$

Definition 2.6.4.3. Intersection (conjunction)

The **intersection** of two fuzzy sets A and B provides a fuzzy set C, which may be represented as $C = A \cap B$ or $C = A$ AND B, its membership function is involved to those of A and B by

$$\mu_C(x) = min(\mu_A(x), \mu_B(x)) = \mu_A(x) \wedge \mu_B(x). \tag{2.39}$$

Definition 2.6.4.4. Complement (negation)

The **complement** of fuzzy set A, shown by $\overline{A}$, (NOT $A, \neg A$), is described as

$$\mu_{\overline{A}}(x) = 1 - \mu_A(x). \tag{2.40}$$

Figure 2.6 shows these three basic operations.

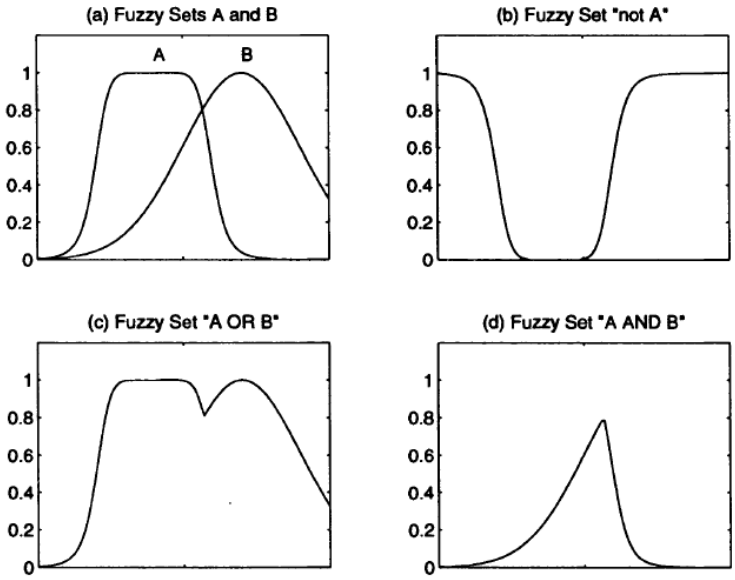

Figure 2.6 Fuzzy sets operations: (a) A and B fuzzy set; (b) not A; (c) union; (d) intersection

Definition 2.6.4.5. Co-product and Cartesian product

The **Cartesian product** of A and B, represented by $A \times B$, is a fuzzy set in the product space $X \times Y$ with the membership function

$$\mu_{A\times B}(x, y) = min(\mu_A(x), \mu_B(y)). \tag{2.41}$$

Similarly, the **Cartesian co-product** $A + B$ is defined with the membership function

$$\mu_{A+B}(x, y) = max(\mu_A(x), \mu_B(y)). \tag{2.42}$$

Both $A \times B$ and $A + B$ are characterized by two-dimensional membership functions.

2.6.5 Membership Function Formulation

The important fuzzy membership functions that are frequently used are as follows

Definition 2.6.5.1. Triangular Membership Functions

Three parameters $\{a, b, c\}$ specify a **triangular membership functions**, as follows:

$$triangle(x; a, b, c) = \begin{cases} 0, & x \leq a. \\ \frac{x-a}{b-a}, & a \leq x \leq b. \\ \frac{c-x}{c-b}, & b \leq x \leq c. \\ 0, & c \leq x. \end{cases} \tag{2.43}$$

By using max and min, an alternative formula is obtained:

$$triangle(x; a, b, c) = max(min(\frac{x-a}{b-a}, \frac{c-x}{c-b}), 0) \tag{2.44}$$

where $a < b < c$.

Definition 2.6.5.2. Trapezoidal Membership Functions

A **trapezoidal membership function** is formalized by four parameters $\{a, b, c, d\}$ as follows:

$$trapezoid(x; a, b, c, d) = \begin{cases} 0, & x \leq a. \\ \frac{x-a}{b-a}, & a \leq x \leq b. \\ 1, & b \leq x \leq c. \\ \frac{d-x}{d-c}, & c \leq x \leq d. \\ 0, & d \leq x. \end{cases} \tag{2.45}$$

Using max and min, alternative formula is obtained:

$$trapezoid(x; a, b, c, d) = max(min(\frac{x-a}{b-a}, 1, \frac{d-x}{d-c}), 0) \tag{2.46}$$

where $a < b \leq c < d$.

Definition 2.6.5.3. Gaussian Membership Function

Two parameters $\{c, \sigma\}$ specify a **Gaussian membership function**:

$$gaussian(x; c, \sigma) = e^{-\frac{1}{2}(\frac{x-c}{\sigma})^2}. \tag{2.47}$$

where c is center and σ is width.

Definition 2.6.5.4. Generalized bell Membership Functiona

A **generalized bell membership function** is formalized by three parameters $\{a, b, c\}$:

$$bell(x; a, b, c) = \frac{1}{1 + |\frac{x-c}{a}|^{2b}}, \tag{2.48}$$

where $b > 0$ (If $b < 0$, it becomes upside-down bell).

Figure 2.7 shows a triangular membership function, trapezoidal membership function, Gaussian membership function, bell membership function described by $triangle(x; 20, 60, 80)$, $trapezoid(x; 10, 20, 60, 95)$, $gaussian(x; 50, 20)$, $bell(x; 20, 4, 50)$, respectively.

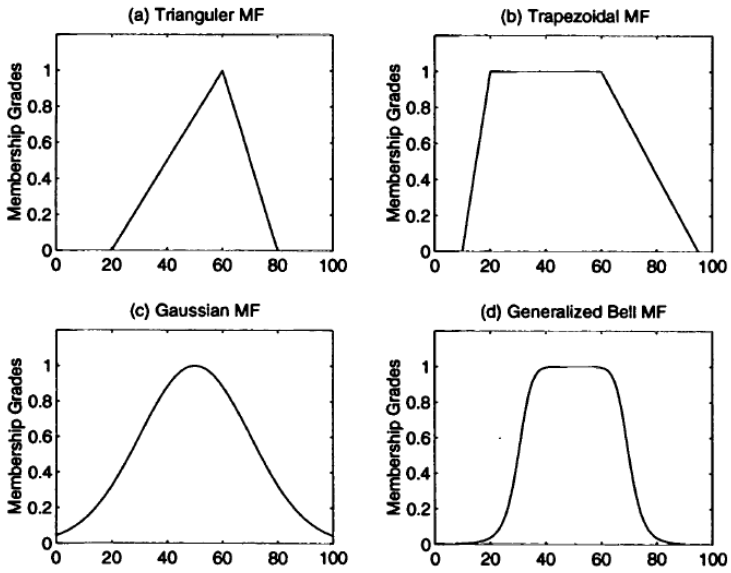

Figure 2.7 Membership function examples

Definition 2.6.5.5. Sigmoidal Membership Functions

A **sigmoidal membership function is defined by**

$$sig(x; a, c) = \frac{1}{1 + exp[-a(x - c)]}, \tag{2.49}$$

where a is slope at the crossover point $x = c$.

Figure 2.8 illustrates two sigmoidal membership functions.

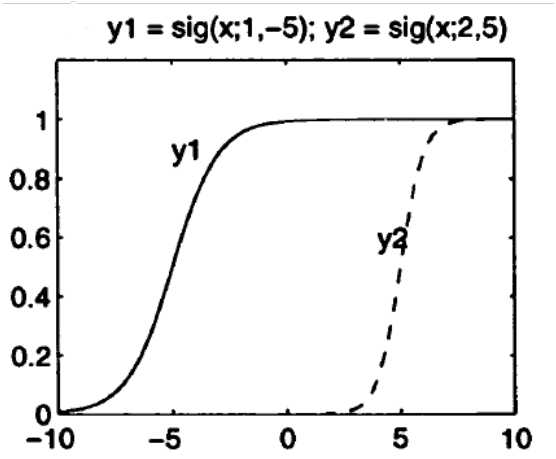

Figure 2.8 Sigmoidal function examples

CHAPTER THREE
CONCEPT: MELANOMA

Melanoma induced skin cancer has been increasing in recent decades. This skin cancer quickly metastasizes when there is no early diagnosis and treatment. In order to perceive the concept of melanoma, it must be understood what the concept of the skin is. Let's overview about the skin.

3.1 The Skin

The largest organ is skin, with a mean weight of 4 kg and a surface $2m^2$area. Its main purpose is to protect the body from the impacts of the outside world by functioning as a barrier against an unwelcoming environment. The significant mortality rate linked with burns that result in severe skin loss highlights the importance of the skin. The epidermis serves as the primary barrier. A vascularized dermis lies beneath the epidermis, providing nutrition and support for the epidermis' dividing cells. Appendages and nerves such as hair follicles, sebaceous glands, and sweat glands are also found in the dermis. Nails are also considered skin appendages. The subcutaneous fat is the deepest and third skin layer (Lookingbill & Marks, 1986). Function and structure are illustrated by skin disease . There exist skin functions, tissue layer and some associated disease in Table 3.1 (Goldsmith, Katz, Bilchrest, Paller, Leffel & Wolff, 2012). Defects in or loss of skin structure disturbs function of skin.

Table 3.1 Functions of skin and some associated diseases

Function	Texture Layer	Diseases
Permeability barrier	1	Keratodermas Exfoliative dermatitis Atopic dermatitis Ectodermal dysplasias Bullous diseases Ichthyoses
Protection from pathogens	1 2	Ecthyma Cellulitis Leishmaniasis Verruca vulgaris Tinea pedis/corporis Human immunodeficiency virus
Thermoregulation	1 2 3	Raynaud Ectodermal dysplasias Hyperthermia
Sensation	1 2 3	Leprosy Pruritus Diabetic neuropathy Postherpetic neuralgia
Ultraviolet protection	1	Oculocutaneous albinism Xeroderma pigmentosum
Wound repair/regeneration	1 2	Venous stasis ulcer Keloid Pyoderma gangrenosum
Physical appearance	1 2 3	Vitiligo Melasma Scleroderma Lipodystrophy

1. Epidermis, 2.Dermis, 3.Hypodermis.

3.1.1 Epidermis

The epidermis is split into four layers, beginning with the basal cell layer at the dermal junction and ending with the stratum corneum at the outer surface Figure 3.1 (Lookingbill & Marks, 1986). The epidermis' dermal side has an irregular form. The downward projections are known as rete ridges, and they look like three-dimensionally as a Gruyere cheese-like matrix with dome-shaped dermal papillae filling the holes. The epidermis is physically attached to the dermis in this configuration (Lookingbill & Marks, 1986).

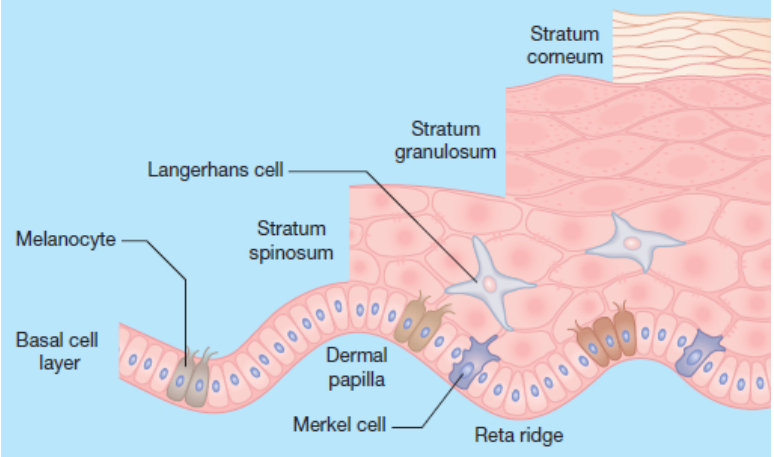

Figure 3.1 Epidermis

The epidermis is a constantly recharhing structure that gives build-up to derivative structures called appendages (nails, sweat glands, and pilosebaceous units) Figure 3.2 (Lookingbill & Marks, 1986).

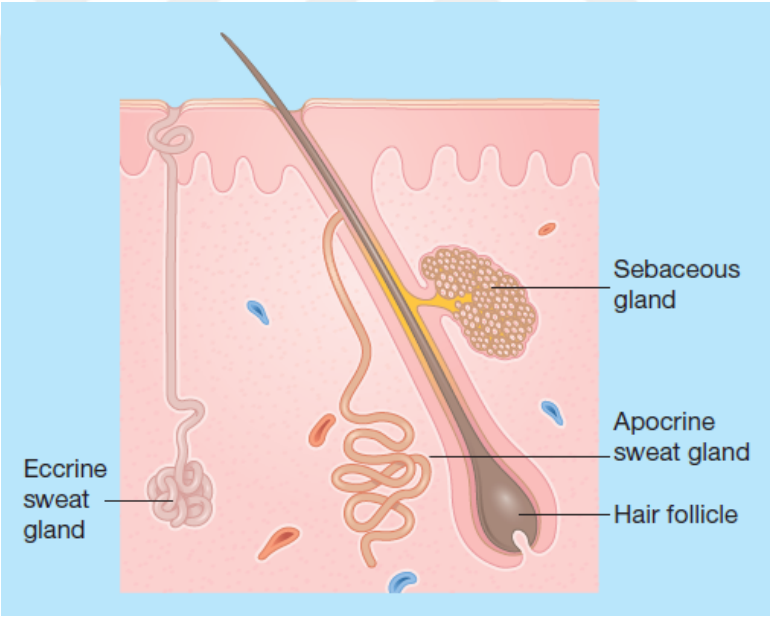

Figure 3.2 Apocrine gland, hair follicle, and sweat gland with sebaceous gland

In comparison to full-thickness skin, which is 1.5 to 4.0 mm thick, the epidermis is 0.4 to 1.5 mm thick. Keratinocytes, which are organized into four layers, make up the majority of cells in the epidermis Figure 3.3 (Goldsmith et al., 2012). From proliferative basal cells connected to the epidermal basement membrane to terminally developed, keratinized stratum corneum, the skin's outermost layer and barrier, these

cells advance. Other cells, such as lymphocytes, are only present for a brief period in the epidermis and are exceedingly uncommon in normal skin. Other cells, such as lymphocytes, are only present in the epidermis for a short time and are extremely rare in normal skin. The epidermis and its appendages have various regional variances (Goldsmith et al., 2012).

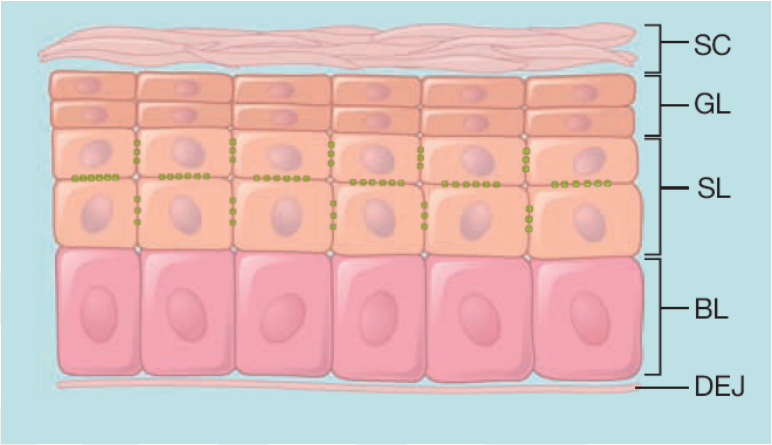

Figure 3.3 Epidermis

3.1.2 Dermis

Nerves, cutaneous, and blood vessels appendages are all found in the dermis, which is a tough, and also elastic support structure. It maintains structural integrity while also being biologically active by interacting with and to regulate cell functions. It is thicker than the epidermis. The dermis thickness may be1 to 4 mm Figure 3.4 (Lookingbill & Marks, 1986).

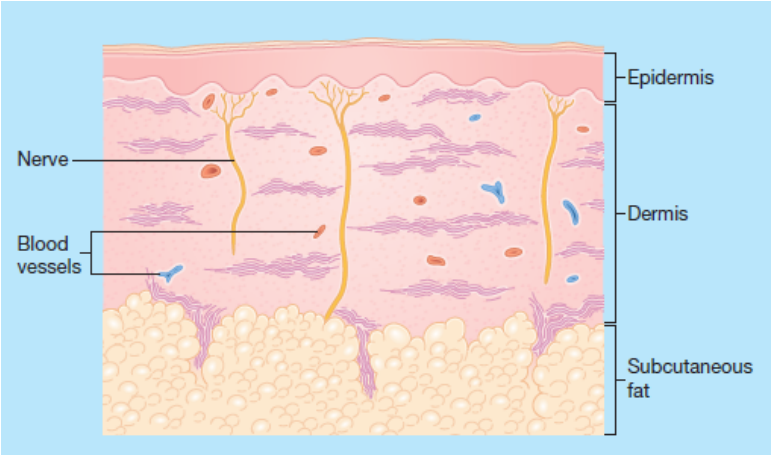

Figure 3.4 Dermis and subcutaneous fat

3.1.3 Skin Appendages and Subcutaneous Fat

Sebaceous glands, hair follicles, nails, and apocrine and eccrine sweat glands consist of skin appendages. They come from the epidermis but, with the exception of nails, are found in the dermis. Eccrine glands aid in body temperature regulation Figure 3.5 (Lookingbill & Marks, 1986).

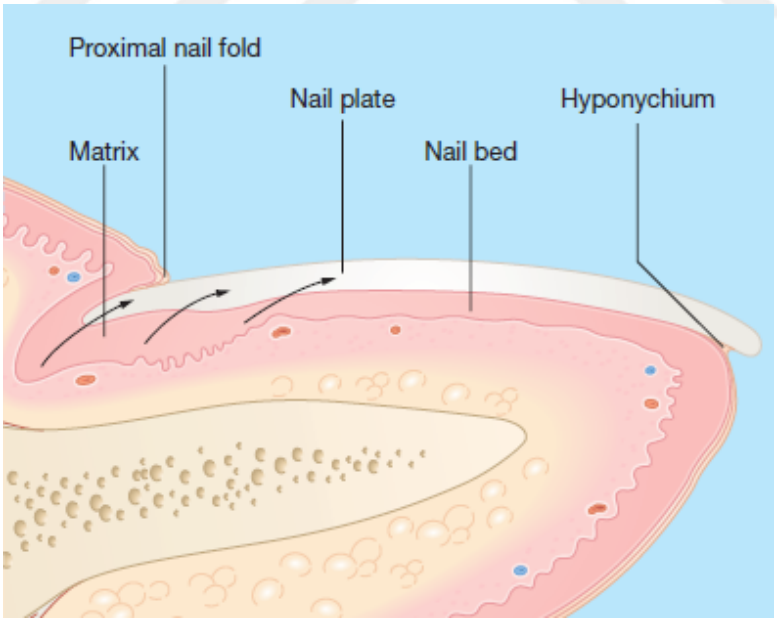

Figure 3.5 Normal nail

Among the underlying fascia and the dermis lies a layer of subcutaneous fat Figure 3.4. It helps to protect the body against cold by acting as a reserve source of

energy. It also protects deep tissues from bruising. Metabolic abnormalities in teenages with insulin resistance and obese children are proof of the significance of biologically active fat cells in hormone signaling. Fibrous septa, at which nerves and blood vessels cross, separates groups of fat cells (lipocytes) (Lookingbill & Marks, 1986).

3.2 Malignacy

The potential for a medical illness to worsen over time is known as malignancy. The term ”malignancy” is most commonly used to describe cancer. Its formal definition is as follows:

“ DNA restore systems protect DNA from mutations that occur often during replication. The cells will proliferate if these systems fail. The outcome is a benign tumour if the growth is gradual and confined to the region where it originates. Otherwise, a malignant tumour will be arised (Encyclopædia Britannica, 2014b).”

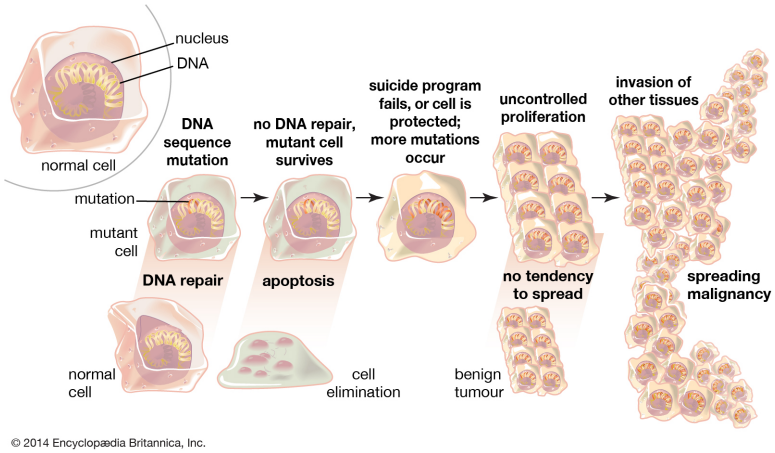

Figure 3.6 Failure of DNA repair mechanisms

3.3 Melanocytes

Melanocytes are pigment-synthesizing dendritic cells that originate from the neural crest and are found mostly in the basal layer Figure 3.7 (Cichorek et al., 2013). Disorders in melanocyte quantity or function have brought attention to the function of melanocytes. The autoimmune loss of melanocytes causes the typical dermatologic disorder vitiligo. Different problems in melanogenesis, including as melanin synthesis, melanosome formation, and melanosome transport and transfer to keratinocytes, are revealed to be the causes of additional pigmentation diseases. The regulation of melanocyte proliferation and homeostasis is being studied in depth as a way to better understood of melanoma. Melanocyte homeostasis and differentiation are influenced by keratinocyte–melanocyte interactions, which dentricity, melanization, and influence proliferation (Goldsmith et al., 2012).

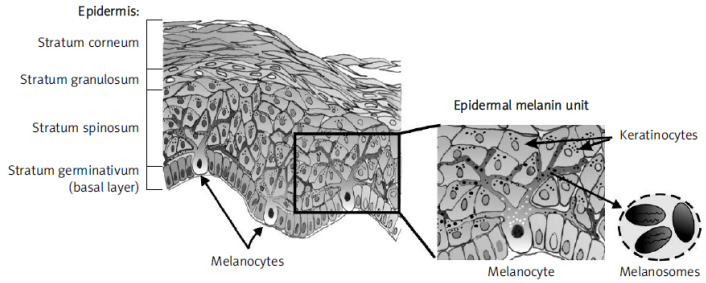

Figure 3.7 Melanocyte

3.4 Melanoma

Melanoma is a form of skin cancer that occurs, when melanocytes get uncontrollably large. When cells grow out of control, cancer develops. Cancerous cells can arise in almost any part of the body and spread to other parts of the body. The risks that cause melanoma formation can be listed as follows:

- Personal History,

- Family History,
- Skin Phenotype,
- Sun Exposure,
- Melanocytic Nevi,
- Genetics.

3.4.1 Clinical Features

A cancerous tumor comprising melanocytes, nevus cells, and pigment-forming cells termed malignant melanoma. It is distinguished clinically by an irregularly shaped and pigmented papule. Melanoma types are passed to the sources as Table 3.2: (1) nodular; (2) acral lentiginous; (3) lentigo maligna; and (4) superficial spreading (Lookingbill & Marks, 1986).

Table 3.2 Melanoma

Type	Location	Median Age (years)	Pre-Metastatic	Frequency (%)*	Ethnicity
Nodular	All surfaces	50	Months to 2 years	9	Caucasian
Acral lentiginous	Palms, soles, nail beds	61	Months to 8 years	1	Black, Asian
Lentigo maligna	Sun-exposed surfaces (head, neck)	70	5–15 years	10	Caucasian
Superficial spreading	All surfaces (back, legs)	47	1–7 years	27	Caucasian

*Unclassified melanomas 53%.

3.4.2 More About Melanoma

Melanocyte stem cells, one possible source of melanoma cells, are found in the bulge area of the hair follicle, an immune-exclusive texture hole with compromised tumor surveillance of immune. Primary melanoma, on the other hand, is only extremely infrequently linked to hair follicles (Bedogni & Paus, 2020) Figure 3.8.

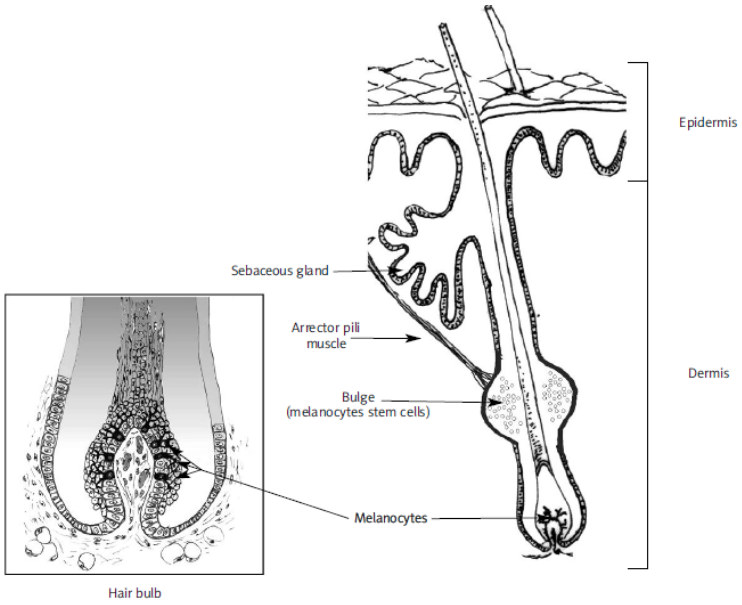

Figure 3.8 Melanocyte localization in the hair

Hair may have a role in the development of melanoma by allowing UVR to penetrate deep into the skin and reach the specialized multipotential stem cell niche in the hair follicle's bulge region. It's worth noting that just a small percentage of melanomas develop directly from the hair follicle (Garcia, McLaren Jr & Meyskens, 2011).

CHAPTER FOUR
CONCEPT: DIGITAL IMAGE PROCESSING

Digital image processing is the technological replication of the human vision system, basically. Whether it is said the power of evolution or the perfection of creation, the human visual system has a perfect structure that has yet to be replicated. As seen in the Figure 4.1 (Drake et al., 2019), the eye consists of 3 basic stages as retina, optic nerves and cortex. In the simplest definition, digital image processing is to imitate the three basic components of the retina, nerves, and cortex. Camera lenses, cables and computer software and algorithms are used instead of these components, respectively.

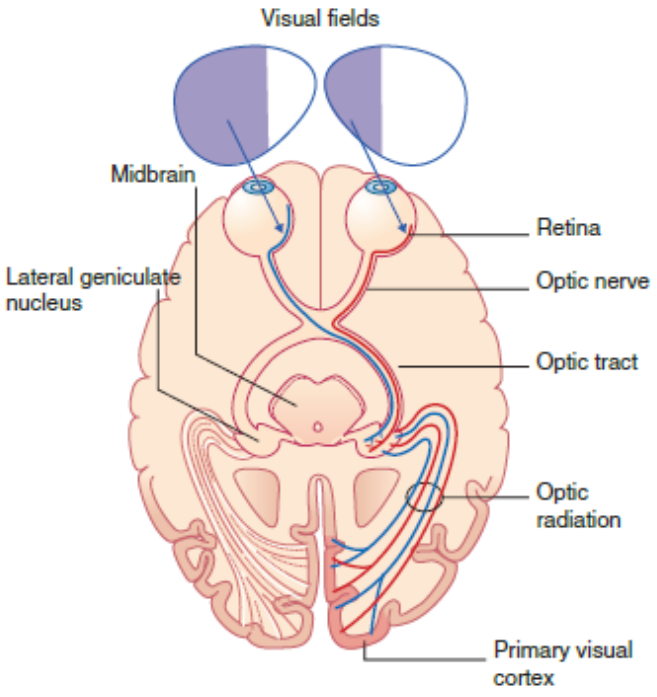

Figure 4.1 Visual pathways: eyes to brain

According to the idea in the Gonzales & Woods (2008), image processing is the inference of some statistical and mathematical formulations of human intuition and analysis based on subjective and visual judgments. The digital acquisition of the image Figure 4.2 (Gonzales & Woods, 2008) is the reduction of the light/energy

emitted from a source to a two-dimensional function as a result of reflection and absorption on the object.

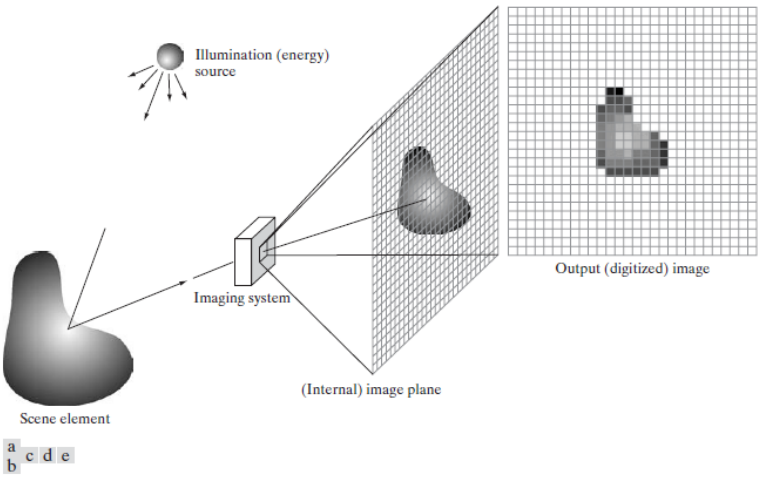

Figure 4.2 Image acquisition (a) energy (b) element (c) imaging system (d) projection (e) image

Digital image processing is applied lots of fields with technological advances, like Space Sciences, Medicine, Industrial Applications, Geographical Information Technologies, Military Applications, Security.

4.1 Basic Definitions About Digital Image Processing

The smallest addressable element in a digital image is called a pixel (pel or picture element). A colour image's pixels have Green, Blue, and Red gray values (Sinecen, 2016).

In Sinecen (2016), there are three different types of pixel neighbour that are 4, 8, and diagonal. Let's define (p) as a pixel that locates by x, y coordinates. The function n defines 8-neighbours of pixel p in Table 4.1.

$N_4(p)$ represents the 4-neighbour of pixel p. There exists two horizontal and two

Figure 4.3 Pixels of a colour image (Sinecen, 2016)

Table 4.1 Neighbor of a pixel

$n(x-1, y-1)$	$n(x-1, y)$	$n(x-1, y+1)$
$n(x, y-1)$	p	$n(x, y+1)$
$n(x+1, y-1)$	$n(x+1, y)$	$n(x+1, y+1)$

vertical neighbours which has unit distance from pixel p. It is shown as follows:

$$N_4(p) = \{n(x, y-1), n(x-1, y), n(x, y+1), n(x+1, y)\} \tag{4.1}$$

$N_D(p)$ represents diagonal neighbours of pixel p. There exists four diagonal neighbours which measures by Euclidean distance. each of them measures by Euclidean distance.

$$N_D(p) = \{n(x-1, y-1), n(x-1, y+1), n(x+1, y+1), n(x+1, y-1)\} \tag{4.2}$$

$N_8(p)$ represents 8-neighbours. It' is a combination of $N_4(p)$ and $N_D(p)$.

$$N_D(p) = \{n(x-1, y-1), n(x-1, y+1), n(x+1, y+1), n(x+1, y-1), \quad (4.3)$$
$$n(x, y-1), n(x-1, y), n(x, y+1), n(x+1, y)\}$$

Two pixels are connected if their gray level values meet a certain requirement and they are neighbors. Adjacency and connection are defined by a collection of intensity values (V). Adjacency can be divided into three categories Figure 4.4 (Sinecen, 2016).

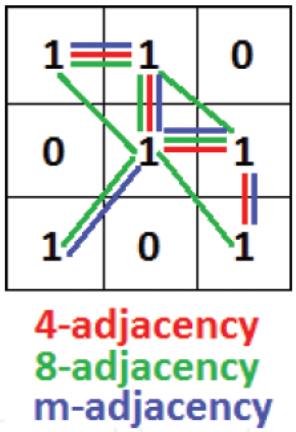

Figure 4.4 Pixel adjacency (Sinecen, 2016)

It is called zoom-in and zoom-out to show details or general view of image, respectively. In this process, resolution changes. Interpolation is used to zoom-in or zoom-out on digital images. The main problem of interpolation is the variation of image resolution Figure 4.5 and Figure 4.6.

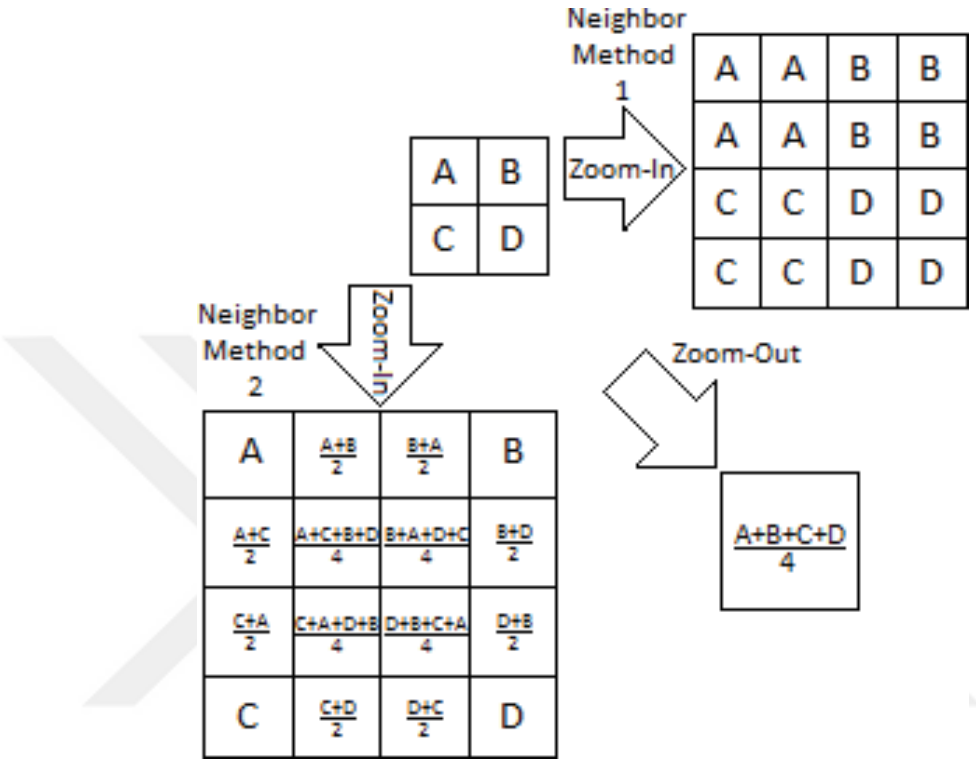

Figure 4.5 Zoom-in and zoom-out (Sinecen, 2016)

Figure 4.6 Image resize (Sinecen, 2016)

4.2 Moreover About Digital Image Processing

Gray Level Co-Occurrence Matrix (GLCM) is one of the best known tools for texture analysis. It is used, widely. It estimates image features in relation to different combinations of gray level changes between binary pixel groups (i, j). Properties such

as energy, entropy, contrast, correlation Table 4.2 which are also known as second order statistical properties and extracted using GLCM, can be used in applications such as image classification and segmentation (Haralick et al., 1973) and (Partio et al., 2002). The GLCM is based on the estimation of the second-order composite state probability density function, $P(i, j|d, \theta)$. This matrix shows the probability of going from gray level i to gray level j when the distance between pixels is d and the angle is θ.

Table 4.2 Some GLCM properties

Property	Function
Contrast	$\sum_{i,j} \|i-j\|^2 p(i,j)$
Correlation	$\sum_{i,j} \frac{(i-\nu i)(j-\nu j)p(i,j)}{\sigma_i \sigma_j}$
Energy	$\sum_{i,j} p(i,j)^2$
Entropy	$\sum_{i,j} \frac{p(i,j)}{1+\|i-j\|}$

CHAPTER FIVE
CONCEPT: ARTIFICIAL NEURAL NETWORKS

Studies on Artificial Neural Networks (ANNs) started with the understanding that the working logic of the brain and the working logic of the traditional computer are completely different. The brain is a nonlinear, parallel information and highly complex processing system. It has the ability to perform certain calculations faster than today's computers by arranging its structural components known as neurons. ANN is a machine designed to model this working principle of the brain (Simon, 1999).

ANNs are used in solving problems belonging to many different disciplines such as mathematics, engineering, physics, computer science, neuroscience and statistics. Due to its learning capability, ANN has found its place in different applications such as signal processing, pattern recognition, forecasting, time series analysis and control.

The operation of the artificial neural network parallels the operation of the biological nerve Figure 5.1. ANN is based on a rough model of the human brain. The neuron is the basic information processing unit in an ANN. Neurons are connected to each other in parallel structure with adjustable weights.

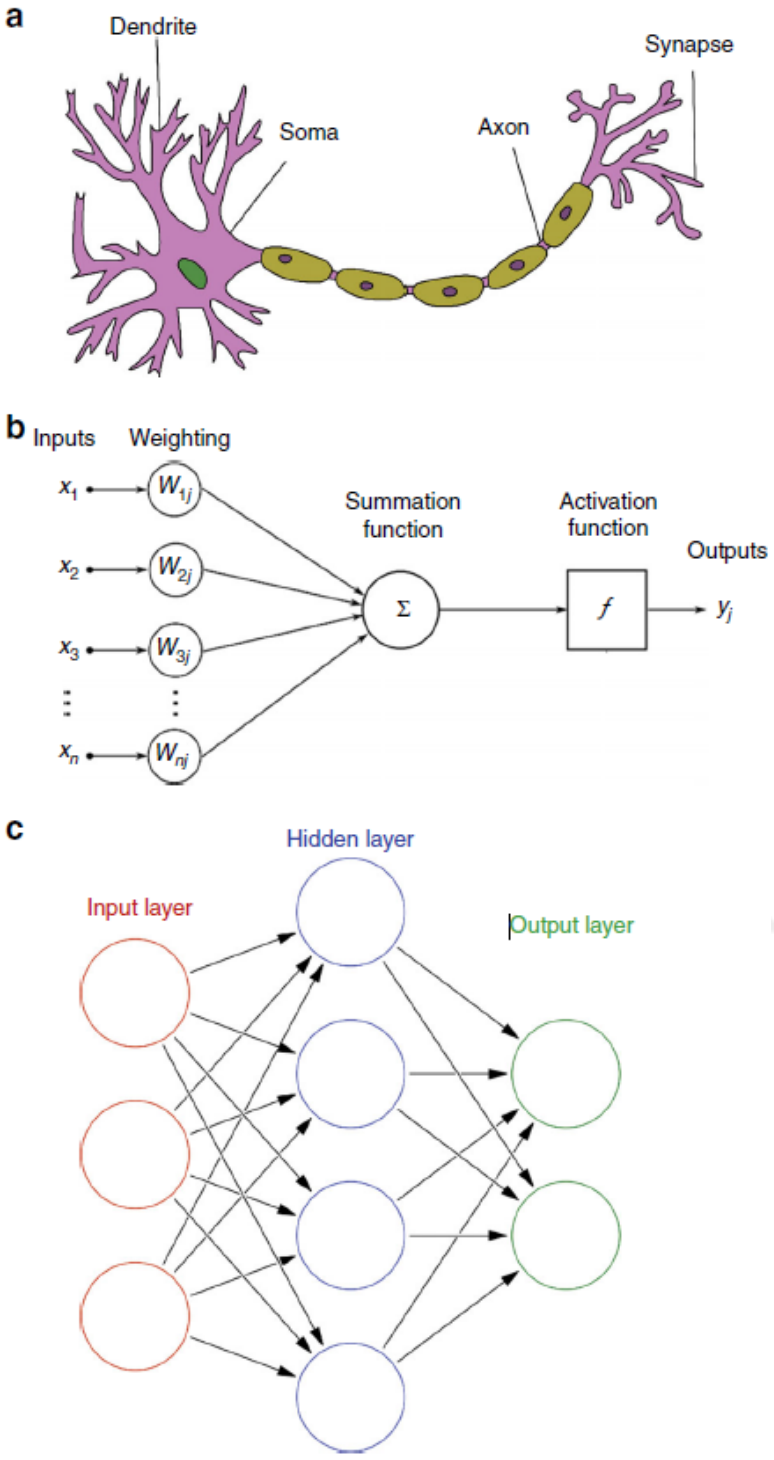

Figure 5.1 ANN working system **a.** biological neurons **b** artificial neurons **c.** ANN (Zhang et al., 2019)

- **Inputs**: Information transmitted from the outside world to the artificial nerve cell.
- **Weights**: A neuron usually receives a lot of input data. Each entry has its own

weight value. Each weight has different fixed values.

- **Summation Function**: It is the function that calculates the net input to a cell.
- **Activation Function**: It is the function that ensures that the net input received by each processing element is processed and the output value corresponding to the input is produced.
- **Outputs**: The result produced by the activation function is considered as cell output. This output is transmitted to other cells to which it is connected according to the location of the cell in the network, or it is evaluated as the result produced by the network.

Thanks to the parallel distributed structure and generalization ability of ANN, its computation and information processing ability is highly developed. Generalization can be defined as being able to produce outputs suitable for examples that the network has never encountered during learning. With these superior features, ANN makes it possible to solve complex problems.

CHAPTER SIX
CONCEPT: APPLICATION

In this chapter, the necessary explanation is made about how the process works and what has been done. The functioning of the process has been discussed in four sections:

- Diagnosis of Melanoma
- Preliminary Study,
- Dataset and Application,
- Results and Discussion.

6.1 Diagnosis of Melanoma

Visual inspection is the most common diagnostic technique. Moles that are irregular in colour or shape are typically treated as candidates. For detection of melanomas to recognize (”ABCD”), to regularly examine moles for changes (shape, size, colour, itching or bleeding) when a candidate appears. This method, which preserves the integrity of the skin compared to biopsy, provides the advantage of not applying any operation to the individual in false positive cases without melanoma. Visual examination is done with a device called dermastoscope in Figure 6.1 (Wikipedia, the free encyclopedia, 2009), which magnifies the skin layer 10-100 times and includes a special optical instrument. This procedure is called dermoscopy. Dermoscopy may cause misdiagnosis depending on factors such as eye health of the examiner.

6.2 Preliminary Study

To understand how to behave Melanoma, a simple simulation is designed using dataset produced by parameters in Table 6.1. To fit the aim of the (Bono et al., 1999)

Figure 6.1 Double polarized dry dermatoscope (Wikipedia, the free encyclopedia, 2009)

study, Four descriptors were chosen to represent the clinical features included in the ABCD rule as follows:

1. *smoothness*,
2. *size*,
3. *mean reflectance*,
4. *roundness*.

For the purpose of (Bono et al., 1999) study, the clinical parameter of asymmetry, borders, colour, dimension were evaluated by roundness, smoothness, mean reflectance, and size, respectively.

Table 6.1 Parameters for nonmelanoma and melanoma lesions

	Cutaneous Melanoma			Other Lesions			
Overall Index Of:	Mean	SD	Median	Mean	SD	Median	P $value^a$
Mean reflectance (ir)	0.36	0.08	0.37	0.43	0.07	0.43	$P < 0.00001$
Mean reflectance(vis)	0.19	0.05	0.18	0.22	0.04	0.21	$P < 0.0001$
Size (mm)	13.38	6.69	13.21	9.59	4.01	9.31	$P < 0.001$
Smoothness	0.87	0.10	0.90	0.92	0.07	0.94	$P < 0.01$
Roundness	0.63	0.16	0.66	0.71	0.12	0.74	$P < 0.01$

Standard deviation(SD); Visible(vis); infrared(ir).
[a] Significance of the OL and CM groups.

In the light of this information, fuzzy inference system is designed with the generated simulation data. Mamdani method is used in the designed system Figure 6.2. The system has 4 inputs as asymmetry, borders, colour, dimension and 1 output as melanoma. It consists of 500 simulated data in such a way that the criteria of the input values are by the Table 6.1. Head of simulated data shows at Table 6.2. 81 rules are used for inference Figure 6.3.

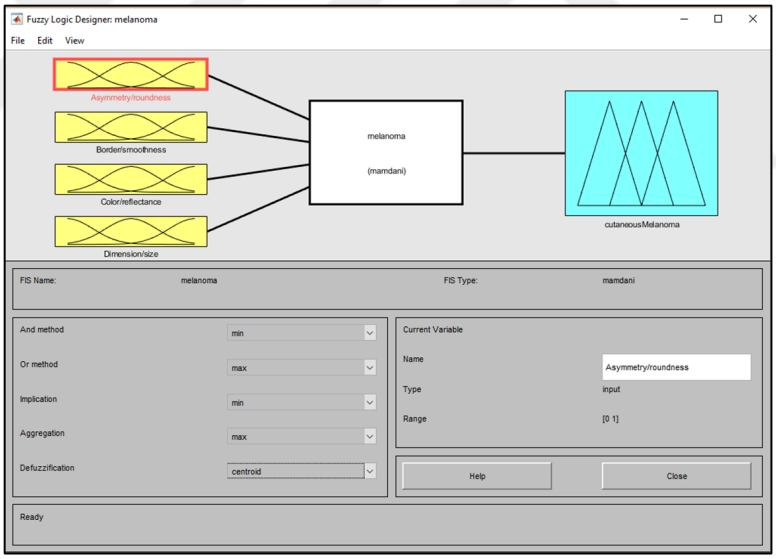

Figure 6.2 Design of fuzzy inference system

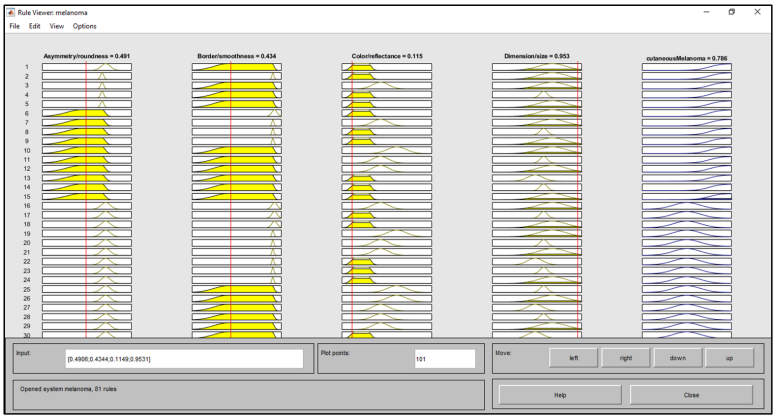

Figure 6.3 Rule page of FIS

Table 6.2 Simulated data

Input A*	Input B**	Input C***	Input D****	Output
0.7	0.4	0.1	0.9	0.8054
0.6	0.5	0.2	0.8	0.8053
0.5	0.6	0.06	0.5	0.7720
0.6	0.5	0.05	0.6	0.5535
0.6	0.5	0.1	0.7	0.7876
0.5	0.6	0.2	0.6	0.8194
0.1	0.2	0.3	0.7	0.6707
0.5	0.3	0.2	0.4	0.8003

*asymmetry,**borders,***colour,****dimension.

Although the results in the study are good, the study has evolved into a new way since the detection of features of melanoma is a separate problem.

6.3 Dataset and Application

The application takes place in 4 basic steps.

1. Preliminary Study,
2. Image Processing,
3. Fuzzy Neural Network,
4. Artificial Neural Network.

To summarize the study briefly, the study is as follows. preliminary study, a fuzzy inference system is created. Afterwards, the FIS is used in the fuzzy neural network. Data from image processing is used in training and testing of the designed fuzzy neural network. In the last step, testing and training are performed with the data from the image processing in the neural network and the outputs are compared.

In an age where data is valuable, obtaining data is a separate problem. However, some limited data sources are available. We used two sources of data. The first one belongs to DermIS database (Dermatology Information System) and the second one belongs to DermQuest database. They obtained from **http://www.dermis.net** and **http://www.dermquest.com** in January 2019, respectively. The Table 6.3 gives us the number of melanoma and nonmelanoma images in the data.

Table 6.3 Number of melanoma

	Melanoma	Nonmelanoma
DermIS	43	26
DermQuest	76	61
Total	119	87

The applications in this thesis are made using the 2020a version of MATLAB. Some features are obtained from 206 images for model training. For this reason, images are resized, specifying that the output images have 256 rows and 256 columns. Gauss filter is used to remove unnecessary details and noise. RGB images are converted to grayscale. In this process, while it is protecting the luminance, it is eliminating the hue and saturation information. The contour of the lesions are determined that using the ready-made functions in the image processing toolbox of MATLAB. Afterwards, the contour of the lesions and the Gaussian filtered RGB images are combined. After this point, some operations are applied to pre-processed and contoured images in order to extract features. Some features have been identified to describe melanoma. Using single-level discrete 2-D wavelet transform, entropy is obtained. Then using Gray-Level Co-Occurrence Matrix, energy, homogeneity and

correlation are obtained. For colour features, mean and standard deviation values are calculated for each RGB level. These images have been analyzed for use in the model and some information was obtained. Image processing method GLCM was used while obtaining the results. Some statistics are given at Table 6.4. The rest of statistics about data is given in appendices section.

Table 6.4 Result of dataset

Entropy	Mean1	Mean2	Mean3	Standard Deviation1	Standard Deviation2	Standard Deviation3	Correlation	Energy	Homogeneity
0.8611	112.6094	98.4199	91.8233	91.9390	80.6382	75.5133	0.9107	0.2317	0.8831
0.9223	45.0482	32.8571	32.7431	72.8349	53.4727	53.1170	0.9471	0.5339	0.9765
0.8439	109.8492	80.4660	72.2471	83.2109	61.9452	55.9272	0.8910	0.3290	0.9317
0.8747	70.4474	57.2056	51.7331	65.9652	54.2309	49.2384	0.8234	0.2519	0.8932
0.8515	75.8177	63.8964	60.0036	62.0191	51.8174	48.6182	0.8905	0.2517	0.9314
0.9473	43.5756	35.6311	32.2402	66.4516	55.5404	49.3569	0.9600	0.4928	0.9742
0.6910	11.6391	13.5907	13.3829	31.2296	33.4757	33.0194	0.9052	0.7046	0.9708
0.7991	30.0224	25.1570	24.4911	59.2952	48.8421	47.6775	0.9574	0.6131	0.9735
0.9998	79.5692	54.8423	54.4721	94.9244	67.8591	66.2408	0.8850	0.3481	0.9296
0.7386	34.7684	22.4069	24.2502	79.3716	51.9160	56.0931	0.9417	0.6769	0.9705

...

206×10 matrix is obtained. A neural network model was designed using ANFIS, which was done as a preliminary study. Model design is shown in Figure 6.4 and Figure 6.5. Table 6.5 describes ANFIS info which used Fuzzy Neural Network (Neuro Fuzzy). Detailed the fuzzy model are available in Figure 6.6 and Figure 6.7. The application of the model working with minimal training RMSE 0.454667 error rate is available in Figure 6.8 and Figure 6.9.

Table 6.5 ANFIS info

Number of nodes	35
Number of linear parameters	9
Number of nonlinear parameters	12
Total number of parameters	21
Number of training data pairs	145
Number of checking data pairs	0
Number of fuzzy rules	9

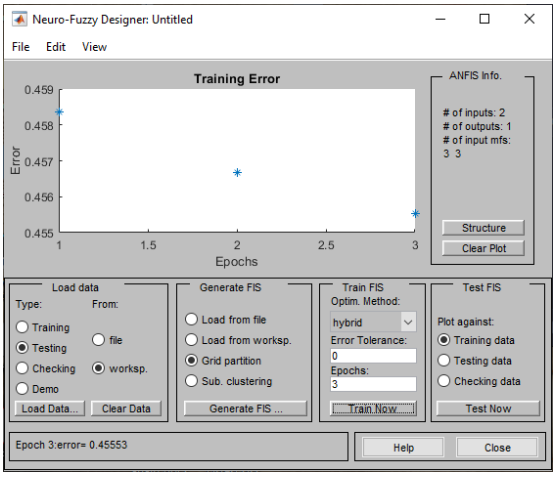

Figure 6.4 General design of Neuro-Fuzzy

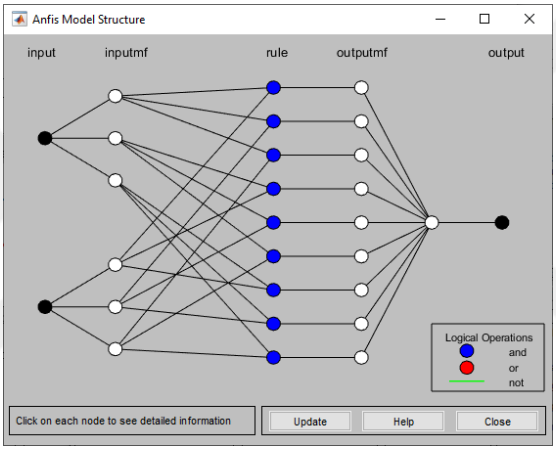

Figure 6.5 ANFIS of NF

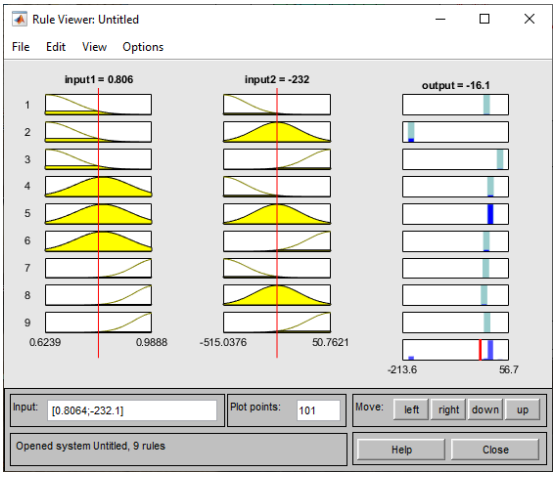

Figure 6.6 Rules of NF

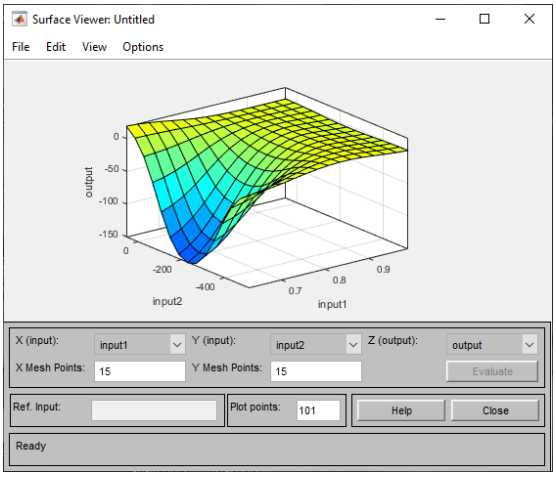

Figure 6.7 Surface view of FIS

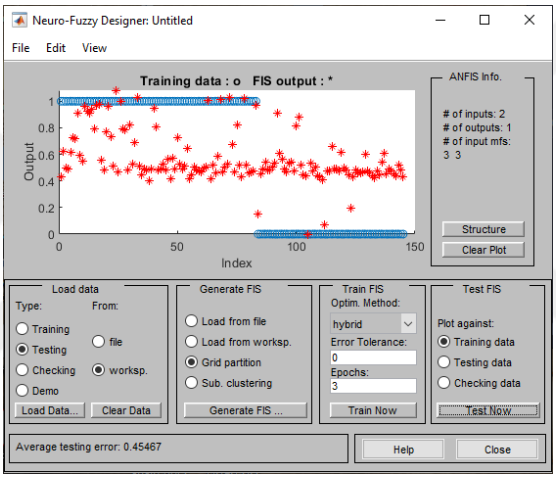

Figure 6.8 Trained model

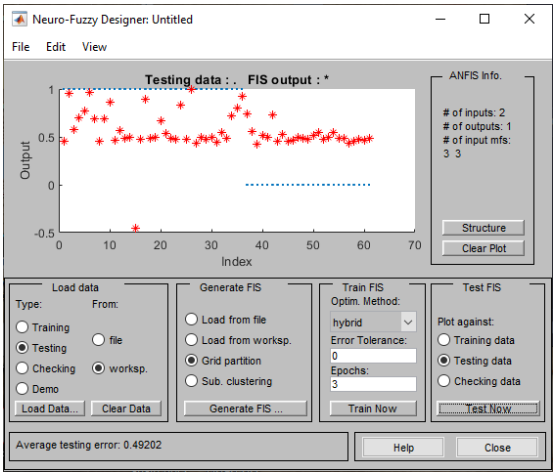

Figure 6.9 Testing model

At the same time, probabilistic neural network is designed with the data obtained as a result of the analysis. It has two layers. The diagonal cells show the number of

true sets that were correctly classified for each class of melanoma Figure 6.11. The number of misclassified residue locations is shown by the number of diagonal cells. The accuracy gained by training the probabilistic neural network utilizing dataset and getting 60.3 percent of data for training as positives is shown in the following results (correctly classified). The ROC curve, the true positive rate versus the false positive rate (sensitivity vs. 1 - specificity) plot is also drawn and shown in Figure 6.10.

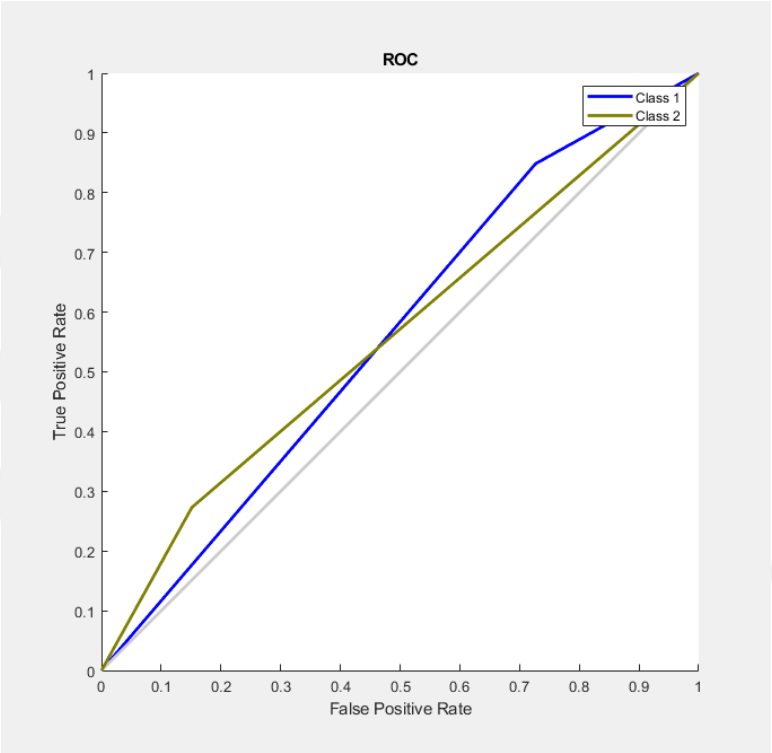

Figure 6.10 ROC curve of designed model

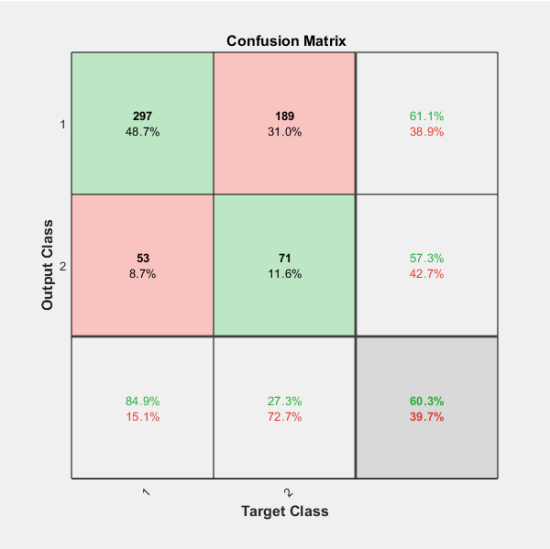

Figure 6.11 Confusion matrix

If it is necessary to exemplify the work, the following figures Figure 6.12, Figure 6.13, Figure 6.14 and Figure 6.15 show the application of the model. The model is tested on four lesions. Three of these lesions are melanoma and one is mole. Results are available Table 6.6.

Table 6.6 Output of application of model

	Entropy	Mean1	Mean2	Mean3	Standard Deviation1	Standard Deviation2	Standard Deviation3	Correlation	Energy	Homogeneity	Output
Lesion1	0.7868	147.7431	120.7231	123.1482	111.3753	91.2231	93.3593	0.8326	0.3274	0.8886	Melanoma
Lesion2	0.5082	186.1335	145.0250	113.1114	74.3850	58.8410	47.5189	0.9333	0.5155	0.9639	Melanoma
Lesion3	0.7281	191.5337	162.0400	162.4254	106.8874	90.5715	91.2900	0.9601	0.3218	0.9621	Melanoma
Lesion4	0.5282	130.6349	117.0641	117.1836	73.4839	66.3326	66.4865	0.8320	0.2486	0.9087	Mole

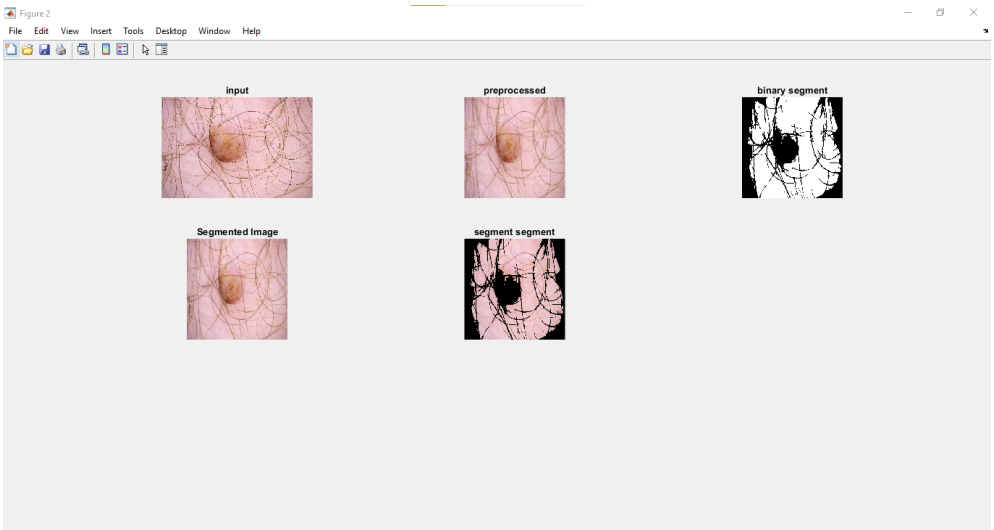

Figure 6.12 Lesion1: melanoma

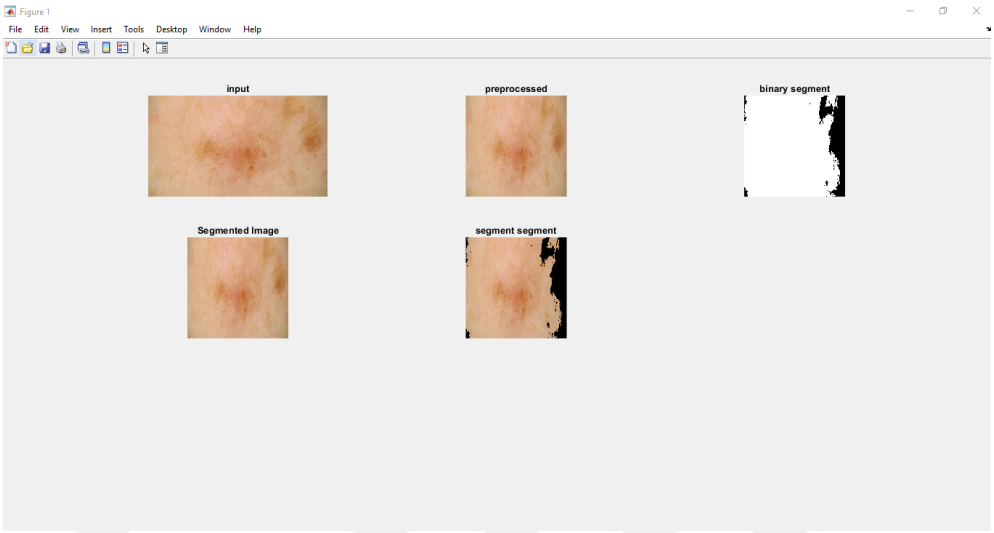

Figure 6.13 Lesion2: melanoma

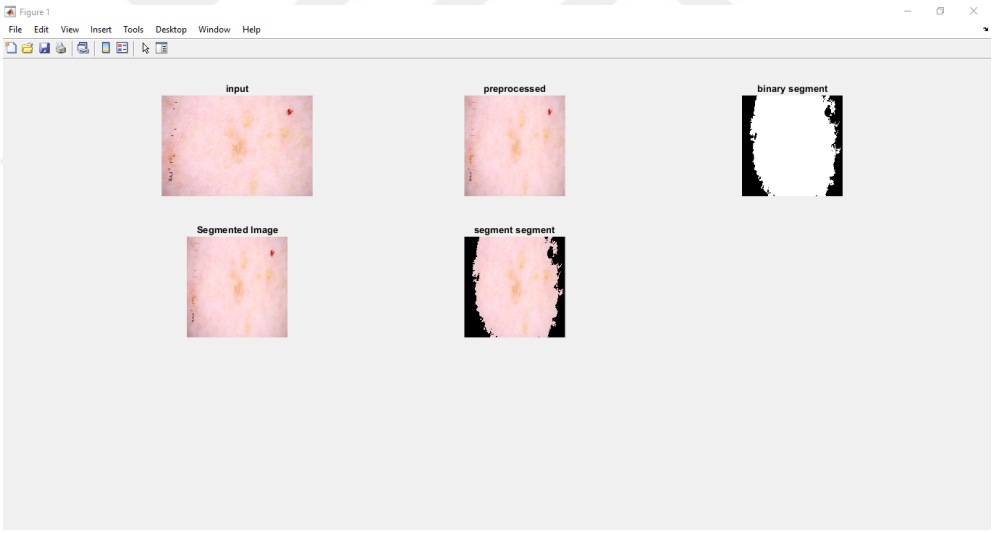

Figure 6.14 Lesion3: melanoma

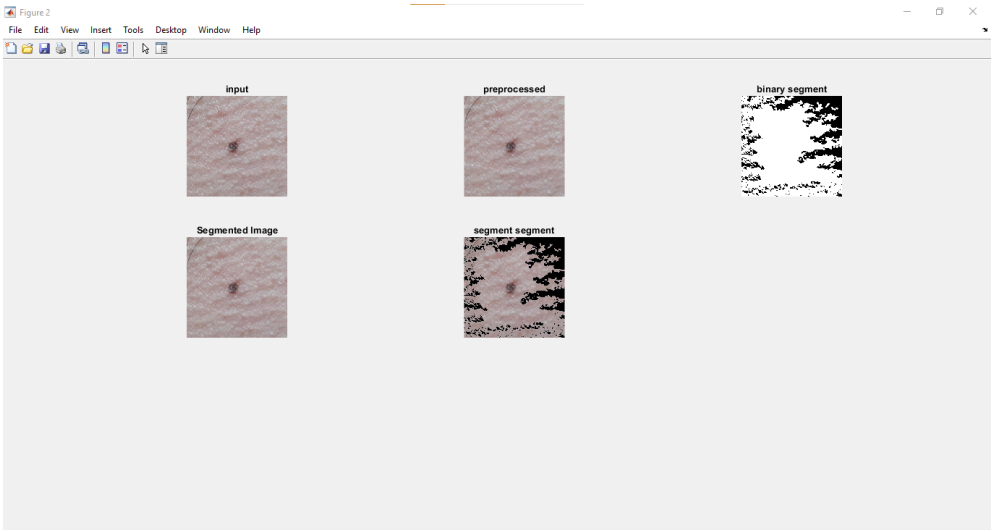

Figure 6.15 Lesion4: mole

6.4 Results and Discussion

In this study, a mixed system was created to be used in the diagnosis of melanoma. As it is known, biopsy is the best method for the diagnosis of melanoma, in most cases it leads to removal of non-melanoma lesions and skin damage. The study is carried out both for early diagnosis and to fully affirm the process with some improvements.

The success rate achieved in the study is 60% for neural network and 55% for fuzzy neural network. If we discuss the reason for this, our first reason is the scarcity of dataset. A data collection study to be carried out at a future date will provide a solution to this problem. After the data collection study will be done, a model can be designed as a validation study of the currently working model.

As a result, in this thesis, a model has been produced in which the use of all functions and parameters is under the control of the user, and a good prediction rate has been achieved. In the future, it is possible to develop this software, train it with more data, and make it available to the medical world.

Studies on methods for detecting and treating melanoma continue. I am confident that better results will be achieved. Don’t forget to apply your sunscreen when you go out in the sun.

CHAPTER SEVEN
CONCLUSION

Diagnosis is based on a patient's signs, symptoms, physical examination, and some tests. However, a single human experience or opportunities may not be enough for the correct diagnosis. Such situations cause problems when doctors make the diagnosis. Developing computer technologies and machine learning techniques are applied to systems that will help doctors in the early diagnosis of diseases. In this study, a decision support system is studied for the detection of melanoma.

In the future, it is possible to develop this software, train it with more data, and make it available to the medical world.

REFERENCES

Almubarak, H. A., Stanley, R. J., Stoecker, W. V., & Moss, R. H. (2017). Fuzzy color clustering for melanoma diagnosis in dermoscopy images. *Information*, *8*(3), 89.

Arroyo, J. L. G., & Zapirain, B. G. (2014). Detection of pigment network in dermoscopy images using supervised machine learning and structural analysis. *Computers in Biology and Medicine*, *44*, 144–157.

Baaz, M., Preining, N., & Zach, R. (2007). First-order gödel logics. *Annals of Pure and Applied Logic*, *147*(1-2), 23–47.

Bedogni, B., & Paus, R. (2020). Hair (y) matters in melanoma biology. *Trends in molecular medicine*, *26*(5), 441–449.

Bolc, L., & Borowik, P. (2013a). *Many-valued logics 1: Theoretical foundations*. Germany: Springer Science & Business Media.

Bolc, L., & Borowik, P. (2013b). *Many-valued logics 1: Theoretical foundations*. Germany: Springer Science & Business Media.

Bono, A., Tomatis, S., Bartoli, C., Tragni, G., Radaelli, G., Maurichi, A., & Marchesini, R. (1999). The abcd system of melanoma detection: A spectrophotometric analysis of the asymmetry, border, color, and dimension. *Cancer: Interdisciplinary International Journal of the American Cancer Society*, *85*(1), 72–77.

Chen, G., Pham, T. T., & Boustany, N. (2001). *Introduction to fuzzy sets, fuzzy logic, and fuzzy control systems*. Florida: CRC Press.

Chung, D. H., & Sapiro, G. (2000). Segmenting skin lesions with partial-differential-equations-based image processing algorithms. *IEEE Transactions on Medical Imaging*, *19*(7), 763–767.

Cichorek, M., Wachulska, M., Stasiewicz, A., & Tymińska, A. (2013). Skin melanocytes: biology and development. *Advances in Dermatology and Allergology/Postępy Dermatologii I Alergologii*, *30*(1), 30.

Colot, O., Devinoy, R., Sombo, A., & de Brucq, D. (1998). A colour image processing method for melanoma detection. In *International Conference on Medical Image Computing and Computer-Assisted Intervention*, (562–569). Germany: Springer.

Drake, R., Vogl, A. W., & Mitchell, A. W. (2019). *Gray's Anatomy for Students*. Amsterdam: Elsevier Health Sciences.

Emre Celebi, M., Kingravi, H. A., Iyatomi, H., Alp Aslandogan, Y., Stoecker, W. V., Moss, R. H., Malters, J. M., Grichnik, J. M., Marghoob, A. A., Rabinovitz, H. S. et al. (2008). Border detection in dermoscopy images using statistical region merging. *Skin Research and Technology*, *14*(3), 347–353.

Encyclopædia Britannica (2014a). *Malignancy*. Retrieved June, 12, 2020, from https://www.britannica.com/science/malignancy#/media/1/360146/58073.

Encyclopædia Britannica (2014b). *Malignancy*. Retrieved June, 12, 2020, from https://www.britannica.com/science/malignancy.

Epstein, G. (1993). *Multiple-valued logic design: an introduction*. Florida: CRC Press.

Ganster, H., Pinz, P., Rohrer, R., Wildling, E., Binder, M., & Kittler, H. (2001). Automated melanoma recognition. *IEEE Transactions on Medical Imaging*, *20*(3), 233–239.

Garcia, A. M. G., McLaren Jr, C. E., & Meyskens, F. L. (2011). Melanoma: is hair the root of the problem? *Pigment cell & melanoma research*, *24*(1), 110.

Garnavi, R., Aldeen, M., & Bailey, J. (2012). Computer-aided diagnosis of melanoma using border-and wavelet-based texture analysis. *IEEE Transactions on Information Technology in Biomedicine*, *16*(6), 1239–1252.

Goldsmith, L. A., Katz, S. I., Bilchrest, B. A., Paller, A. S., Leffel, D. J., & Wolff, K. (2012). *Fitzpatrick's Dermatology in General Medicine* (8th ed.). New York: The McGraw-Hill Companies.

Gonzales, R. C., & Woods, R. E. (2008). *Digital image processing 3rd ed*. Upper Saddle River: Prentice Hall International.

Gottwald, S. (2015). The logic of fuzzy set theory: a historical approach. In *Petr Hájek on Mathematical Fuzzy Logic* (41–61). Germany: Springer.

Grossniklaus, H. E. (2013). Progression of ocular melanoma metastasis to the liver: the 2012 zimmerman lecture. *JAMA Ophthalmology*, *131*(4), 462–469.

Haralick, R. M., Shanmugam, K., & Dinstein, I. H. (1973). Textural features for image classification. *IEEE Transactions on Systems, Man, and Cybernetics*, (6), 610–621.

Hoshyar, A. N., Al-Jumaily, A., & Hoshyar, A. N. (2014). Comparing the performance of various filters on skin cancer images. *Procedia Computer Science*, *42*, 32–37.

Jain, S., Pise, N. et al. (2015). Computer aided melanoma skin cancer detection using image processing. *Procedia Computer Science*, *48*, 735–740.

Jang, J.-S. R., Sun, C.-T., & Mizutani, E. (1997). Neuro-fuzzy and soft computing-a computational approach to learning and machine intelligence [book review]. *IEEE Transactions on Automatic Control*, *42*(10), 1482–1484.

José Costa (2020). *Milestones In Cancer Science*. Retrieved February, 24, 2020 from https://www.britannica.com/science/cancer-disease/Milestones-in-cancer-science.

Karpenko, A. S. (2006). *Lukasiewicz's logics and prime numbers*. UK: Luniver Press.

Lin, J. Y., & Fisher, D. E. (2007). Melanocyte biology and skin pigmentation. *Nature*, 843-850.

Lookingbill, D. P., & Marks, J. G. (1986). *Principles of dermatology*. Philadelphia: Saunders.

Partio, M., Cramariuc, B., Gabbouj, M., & Visa, A. (2002). *Rock texture retrieval using gray level co-occurrence matrix 5th ed.* Pennsylvania: Citeseer.

Rajab, M., Woolfson, M., & Morgan, S. (2004). Application of region-based segmentation and neural network edge detection to skin lesions. *Computerized Medical Imaging and Graphics*, *28*(1-2), 61–68.

Ruiz, D., Berenguer, V., Soriano, A., & Sánchez, B. (2011). A decision support system for the diagnosis of melanoma: A comparative approach. *Expert Systems with Applications*, *38*(12), 15217–15223.

Schmid-Saugeona, P., Guillodb, J., & Thirana, J.-P. (2003). Towards a computer-aided diagnosis system for pigmented skin lesions. *Computerized Medical Imaging and Graphics*, *27*(1), 65–78.

Shakespeare, W. (1912). *Hamlet*. UK: Clarendon Press.

Simon, H. (1999). *Neural networks: a comprehensive foundation*. New Jersey: Prentice Hall.

Sinecen, M. (2016). Digital image processing with matlab. In J. Valdman (Ed.), *Applications from Engineering with MATLAB Concepts* chapter 1, (1-43). London: IntechOpen Limited.

Soh, L.-K., & Tsatsoulis, C. (1999). Texture analysis of sar sea ice imagery using gray level co-occurrence matrices. *IEEE Transactions on Geoscience and Remote Sensing*, *37*(2), 780–795.

Sumithra, R., Suhil, M., & Guru, D. (2015). Segmentation and classification of skin lesions for disease diagnosis. *Procedia Computer Science*, *45*, 76–85.

The Surveillance, Epidemiology, and End Results (2021). *5-years Survival Rate*. Retrieved May, 4, 2021 from https://seer.cancer.gov/statfacts/html/melan.html.

Wikipedia, the free encyclopedia (2009). *Dermatoscope*. Retrieved December, 27, 2020, from https://en.wikipedia.org/wiki/File:Dermatoscope1.JPG.

Zadeh, L. A. (1965). Fuzzy sets. *Information and control*, *8*(3), 338–353.

Zhang, Q., Yu, H., Barbiero, M., Wang, B., & Gu, M. (2019). Artificial neural networks enabled by nanophotonics. *Light: Science & Applications*, *8*(1), 1–14.

Zimmermann, H.-J. (2010). Fuzzy set theory. *Wiley Interdisciplinary Reviews: Computational Statistics*, *2*(3), 317–332.

APPENDICES

Table A.1 Result of dataset

Entropy	Mean1	Mean2	Mean3	Standard Deviation1	Standard Deviation2	Standard Deviation3	Correlation	Energy	Homogeneity
0.8611	112.6094	98.4199	91.8233	91.9390	80.6382	75.5133	0.9107	0.2317	0.8831
0.9223	45.0482	32.8571	32.7431	72.8349	53.4727	53.1170	0.9471	0.5339	0.9765
0.8439	109.8492	80.4660	72.2471	83.2109	61.9452	55.9272	0.8910	0.3290	0.9317
0.8747	70.4474	57.2056	51.7331	65.9652	54.2309	49.2384	0.8234	0.2519	0.8932
0.8515	75.8177	63.8964	60.0036	62.0191	51.8174	48.6182	0.8905	0.2517	0.9314
0.9473	43.5756	35.6311	32.2402	66.4516	55.5404	49.3569	0.9600	0.4928	0.9742
0.6910	11.6391	13.5907	13.3829	31.2296	33.4757	33.0194	0.9052	0.7046	0.9708
0.7991	30.0224	25.1570	24.4911	59.2952	48.8421	47.6775	0.9574	0.6131	0.9735
0.9998	79.5692	54.8423	54.4721	94.9244	67.8591	66.2408	0.8850	0.3481	0.9296
0.7386	34.7684	22.4069	24.2502	79.3716	51.9160	56.0931	0.9417	0.6769	0.9705
0.9099	36.1552	23.3121	21.8919	57.7094	38.8807	37.2616	0.9298	0.4970	0.9611
0.8802	24.6166	17.7703	20.5832	49.9088	36.0023	41.1933	0.8841	0.6035	0.9602
0.8974	40.9296	38.2737	41.0384	67.7017	63.1797	67.7249	0.9436	0.5160	0.9426
0.9982	41.8662	31.3387	51.8452	48.5988	36.1252	54.9138	0.8794	0.3032	0.9187
0.8993	21.3883	23.1422	23.2204	38.7170	40.1050	39.6633	0.9172	0.5196	0.9465
0.8216	13.4924	14.1289	15.3857	29.3476	28.0154	30.2189	0.8582	0.6154	0.9580
0.8212	18.3807	14.8172	13.4678	36.4375	29.3192	26.4185	0.8996	0.6104	0.9674
0.7034	14.8823	14.5375	13.0974	36.8988	35.1385	32.3712	0.8959	0.6995	0.9663
0.8691	17.8276	15.9066	16.6887	35.5785	32.2009	33.6695	0.8583	0.5984	0.9583
0.7623	20.3331	17.4592	14.3144	49.2817	41.7899	34.4361	0.8998	0.6946	0.9682
0.7905	22.8156	21.2448	17.4915	46.5115	43.3868	36.6718	0.9170	0.6202	0.9582
0.9127	33.6604	27.9132	24.3539	62.0793	51.4168	43.7101	0.9144	0.5642	0.9615
0.4884	6.8402	7.9543	8.8575	24.2080	26.7679	29.5997	0.8697	0.8236	0.9739
0.6108	12.7211	11.2711	10.1721	36.1893	32.6421	28.8357	0.8984	0.7554	0.9713
0.9991	57.2423	49.9232	45.6105	72.8544	64.6840	59.2232	0.8900	0.4302	0.9519
0.7654	116.0953	95.0523	80.5618	88.2053	72.8685	62.7649	0.8635	0.2339	0.8678
0.8155	138.7820	124.8425	116.2289	95.3285	86.0531	80.0347	0.9344	0.2392	0.9101
0.8275	23.6864	22.4643	20.6326	46.6549	42.2796	39.1454	0.9171	0.5871	0.9550
0.5704	10.5882	10.3811	10.9292	32.6098	30.4153	31.6729	0.9003	0.7816	0.9761
0.8308	31.7937	24.2840	21.5279	61.3263	47.5411	42.4367	0.9371	0.6093	0.9709
0.6276	161.9093	155.7712	140.1532	89.3708	86.0561	77.7602	0.9049	0.4071	0.9227
0.7013	16.4449	13.2000	13.1281	37.1243	30.2861	30.3117	0.9296	0.6944	0.9798
0.6697	107.9870	86.7523	74.2692	69.9980	56.7940	48.9590	0.8601	0.3185	0.9274
0.6235	13.6984	11.2593	11.4832	40.1257	32.7592	33.4291	0.8720	0.7734	0.9714
0.8508	25.1603	19.8178	20.1300	49.9689	39.7737	40.0157	0.8633	0.5991	0.9474
0.5339	9.5130	8.9298	9.1141	27.9947	26.4160	27.2658	0.9249	0.7872	0.9810
0.9783	74.4948	65.3699	59.9158	85.2921	76.4611	70.3633	0.8180	0.3132	0.8907
0.9120	31.0311	27.5417	24.7047	62.9125	55.9242	50.0002	0.8700	0.5960	0.9449
0.4521	9.0532	6.5806	6.7045	31.0578	23.2431	23.6862	0.9061	0.8372	0.9818
0.9932	64.5569	56.2855	54.2103	81.6427	72.3457	68.5911	0.9360	0.3889	0.9492
0.4568	6.4479	6.1910	6.7895	23.5887	22.1019	24.3105	0.8799	0.8406	0.9784
0.9562	27.8420	27.9884	27.2157	42.7104	41.9469	40.8412	0.9135	0.4512	0.9436
0.6235	18.6108	13.2510	12.6109	49.6561	36.0533	33.6475	0.9451	0.7541	0.9836
0.8355	161.6652	131.5006	111.6961	113.1697	94.3554	81.5022	0.9636	0.2330	0.9475
0.8637	75.5335	39.2647	41.6693	58.2520	33.6515	35.9021	0.8670	0.1961	0.9050
0.9898	72.4550	46.8647	32.3595	73.7559	48.6973	34.2674	0.9164	0.3034	0.9482
0.6931	147.8370	97.4547	73.6548	86.4113	58.4638	45.3457	0.9236	0.2326	0.9019
0.9608	75.3315	57.6522	50.7943	76.1020	59.2645	53.1257	0.8780	0.2695	0.9051
0.8598	129.3411	106.1127	96.6504	97.8161	80.8662	74.3989	0.9495	0.2114	0.9063
0.8946	123.2738	97.2089	83.8600	96.8010	77.2769	68.0810	0.9418	0.2374	0.9107
0.6772	154.6883	109.0679	91.5961	86.1246	62.6819	54.7311	0.9587	0.1453	0.8986
0.9630	98.5375	70.7342	64.7808	91.7499	67.0157	62.1393	0.9687	0.2426	0.9171
0.5704	197.7509	168.9369	142.5257	89.1629	77.2497	65.5795	0.9618	0.2444	0.9397
0.5039	4.2719	2.6597	2.6248	16.8433	12.3042	12.5810	0.7153	0.9208	0.9853
0.9284	31.1189	17.9089	13.9805	52.2469	31.8018	24.8669	0.9012	0.5548	0.9673
0.9050	126.9573	89.1991	74.5375	95.7628	68.6098	58.0401	0.9740	0.2300	0.9368

...

Table A.1 continues

Entropy	Mean1	Mean2	Mean3	Standard Deviation1	Standard Deviation2	Standard Deviation3	Correlation	Energy	Homogeneity
0.6312	191.2778	171.0686	160.1226	99.9084	90.4549	84.6733	0.9242	0.2756	0.9304
0.9947	74.7272	60.0396	42.5951	82.6621	66.6812	48.6551	0.9363	0.3428	0.9413
0.7174	159.2158	125.4381	98.9828	90.2238	71.8036	57.5533	0.9543	0.2859	0.9166
0.9925	62.1702	49.6943	45.5053	88.1793	69.3545	62.7864	0.8938	0.4113	0.9158
0.6513	158.7375	129.6081	115.5132	83.2637	68.8373	62.9594	0.9297	0.1988	0.8867
0.9462	72.0842	51.3153	42.3365	63.4619	45.3044	37.8510	0.9247	0.2767	0.9494
0.8617	126.0070	98.8563	88.0619	94.7534	75.1462	67.5016	0.9350	0.2382	0.9097
0.8627	32.6381	25.3309	20.4629	75.3992	59.3880	47.8182	0.8499	0.6754	0.9544
0.7019	166.8125	137.5275	109.1087	98.5254	82.4373	66.5555	0.9282	0.2262	0.9006
0.8852	137.6804	100.0884	77.1620	101.0361	73.6103	57.0125	0.9720	0.3129	0.9576
0.9999	68.8453	58.3614	53.3124	82.7207	70.6843	64.6897	0.9228	0.3885	0.9463
0.7570	161.0870	132.3692	109.3633	97.6166	82.9626	69.2041	0.9570	0.1768	0.9082
0.9763	62.3915	45.6739	35.9997	65.6515	48.4220	38.7913	0.8924	0.3112	0.9296
0.5697	9.4904	8.6669	7.8544	31.9622	28.4426	25.6586	0.8876	0.8139	0.9769
0.9985	46.6669	29.9620	20.9323	59.4749	40.0091	28.9474	0.9246	0.4033	0.9487
0.6697	168.2409	154.4011	145.8154	104.0715	95.8896	90.6311	0.8657	0.2654	0.8915
0.9958	69.0982	42.5042	30.2585	80.8720	50.9646	36.7807	0.8840	0.3523	0.9347
0.5960	144.3170	107.4951	89.4551	85.6444	64.4010	54.0215	0.8138	0.2018	0.8381
0.9811	92.3756	69.7752	53.7375	99.6837	75.6974	58.6921	0.9455	0.3410	0.9511
0.7926	142.8414	107.2744	79.2319	98.4981	74.4812	55.3751	0.9271	0.3012	0.9163
0.9677	80.7336	57.0044	45.0622	75.1929	54.9553	44.3799	0.9081	0.2751	0.9409
0.9925	73.1644	56.5250	46.3114	84.0994	65.3000	53.3677	0.9144	0.4075	0.9519
0.9876	109.3134	85.8007	71.0670	109.3795	85.9765	71.3094	0.9662	0.3445	0.9576
0.9372	97.4637	61.5112	48.8444	93.9732	60.3210	48.6792	0.8726	0.2888	0.9043
0.7520	168.8382	106.7224	89.1052	96.9420	62.4453	52.7870	0.9639	0.2897	0.9431
0.9242	135.3558	110.1945	99.4684	104.8267	86.6846	78.9338	0.9892	0.2517	0.9672
0.8825	143.7479	118.5972	108.9586	99.5630	82.9479	76.8341	0.9941	0.2447	0.9750
0.9920	102.6896	69.3547	56.0276	102.2345	69.4838	56.8241	0.9745	0.3095	0.9447
0.9955	103.3762	67.9163	53.0591	104.8306	69.3979	54.8748	0.9763	0.3236	0.9485
0.7100	21.4294	11.7359	7.9784	47.1564	27.0284	18.7387	0.9183	0.6807	0.9763
0.8935	140.0620	116.7450	99.6102	108.7608	92.3721	79.7369	0.9625	0.2598	0.9511
0.8238	20.4299	8.8432	7.5607	43.0942	21.4047	18.7345	0.7755	0.6629	0.9582
0.5304	169.0108	114.2452	104.7921	77.2066	58.8688	55.3432	0.9599	0.1708	0.9200
0.8568	7.7374	9.0816	9.6491	22.2136	20.1548	20.3714	0.7537	0.7567	0.9617
0.9999	74.4268	58.4787	55.4872	83.3331	68.1630	65.3066	0.9334	0.3577	0.9436
0.9216	100.2390	80.1610	71.1445	93.9905	76.2474	68.7243	0.9121	0.2278	0.8441
0.9967	57.7590	40.5562	31.3555	74.2429	55.1836	43.7682	0.9061	0.3914	0.9455
0.7801	145.3047	116.6403	96.2498	106.7172	86.7851	71.9618	0.8951	0.2281	0.8921
0.6713	14.8795	6.3769	5.7104	35.7667	17.7736	15.9313	0.8412	0.7339	0.9744
0.7013	153.7238	112.5842	89.0939	84.5535	64.6829	52.3887	0.9771	0.2001	0.9346
0.8474	156.1248	122.5464	109.7774	106.4026	84.1900	75.6798	0.9793	0.2985	0.9727
0.9830	88.5553	71.2089	66.9557	86.0752	69.6745	66.0048	0.9220	0.3086	0.9376
0.9941	71.4589	53.3880	52.4056	85.5685	66.7171	65.8901	0.9478	0.3610	0.9481
0.8542	138.8596	122.2678	115.8391	94.7742	84.5723	80.5865	0.9744	0.2183	0.9307
0.9722	76.7426	52.3949	41.4777	78.8143	55.6138	45.6806	0.8934	0.2636	0.9087
0.6746	8.5536	7.0527	6.5444	26.1434	20.3816	18.7343	0.7504	0.7921	0.9680
0.5710	143.4778	103.2376	99.3346	87.2724	63.6348	61.4639	0.8274	0.1604	0.8232
0.7252	152.2358	126.0297	131.4587	95.0476	79.5044	82.7720	0.9423	0.1907	0.8867
0.8170	113.1815	71.1727	79.8030	90.7476	58.9222	66.1893	0.8408	0.2518	0.8777
0.7958	145.8398	105.6658	89.4409	96.4795	73.6897	64.3293	0.9497	0.1682	0.9078
0.8681	132.4047	106.3962	102.5928	104.1078	84.1969	81.5962	0.9484	0.2016	0.8913
0.9837	70.6518	55.3891	53.7478	75.4374	60.7297	58.3629	0.8976	0.3151	0.9227
0.9004	60.0575	46.9898	35.5917	52.8116	45.9858	35.7657	0.9202	0.2857	0.9371
0.9031	111.1745	83.7085	72.4789	94.7023	73.2360	64.9805	0.9275	0.2047	0.8582
0.8927	31.2774	24.5091	23.5117	59.7025	47.1957	45.7302	0.9174	0.5921	0.9649
0.4607	4.7476	3.1452	3.7989	18.1228	12.3232	14.1083	0.7077	0.8825	0.9833
0.8703	69.6486	46.9180	35.4130	62.2673	41.9651	32.6807	0.8832	0.2270	0.9174
0.8470	24.7353	19.3021	17.1773	51.5404	41.6453	37.1290	0.8895	0.6504	0.9619
0.8140	112.2126	82.0790	69.7422	94.3560	70.1308	60.6513	0.8059	0.2157	0.8254
0.8027	120.0418	81.4504	67.4560	89.5123	61.5129	51.5398	0.8666	0.2454	0.8605

...

Table A.1 continues

Entropy	Mean1	Mean2	Mean3	Standard Deviation1	Standard Deviation2	Standard Deviation3	Correlation	Energy	Homogeneity
0.8223	155.6206	123.6641	93.0096	104.1456	84.4139	64.4792	0.9553	0.2619	0.9454
0.7538	18.7542	15.8531	13.8641	41.3701	35.0092	31.5482	0.8916	0.6563	0.9600
0.8163	13.7961	7.4917	6.5445	30.0395	17.8994	15.7437	0.8112	0.7475	0.9696
0.6708	128.8194	124.3879	118.1858	70.2793	68.3645	64.5093	0.9294	0.2860	0.9237
0.8774	21.2153	23.5646	23.6093	46.4212	50.4069	50.3288	0.8747	0.6466	0.9656
0.8062	107.5781	83.0284	70.6523	79.2975	61.0752	53.5429	0.9275	0.2288	0.9140
0.3477	79.6263	53.1079	48.6592	38.9362	24.8150	23.9421	0.8596	0.2922	0.9335
0.9921	59.0874	53.3883	50.1180	65.8752	60.0900	56.7389	0.9339	0.4296	0.9573
0.9610	53.0879	49.7516	41.3718	78.4165	73.5395	60.8691	0.9462	0.4718	0.9552
0.7447	147.1764	99.1425	66.8858	86.9376	58.5399	39.5806	0.9338	0.3894	0.9419
0.8840	78.6279	70.4222	66.5795	72.4412	66.0988	62.5748	0.8458	0.3223	0.9249
0.9959	75.2723	68.6984	68.1785	93.2237	85.7008	85.1981	0.9642	0.3815	0.9329
0.6772	146.4938	118.4201	99.2875	86.5158	70.9120	62.6880	0.9296	0.1975	0.9006
0.9696	107.9935	58.5920	36.3267	99.5495	54.6754	34.8407	0.9244	0.3445	0.9501
0.9326	114.0981	77.9504	53.7994	96.3746	67.0378	48.1102	0.9455	0.3264	0.9530
0.9968	77.8783	51.7419	36.6012	85.5007	58.5203	44.3669	0.9505	0.3789	0.9634
0.4269	4.2561	3.6909	3.3437	18.3203	14.5778	12.7365	0.8521	0.8862	0.9888
0.7822	106.3304	105.1989	103.3150	75.0312	74.5458	73.2947	0.8680	0.2243	0.8908
0.7442	21.5973	16.4797	13.7349	49.8349	38.3903	32.2219	0.8877	0.6966	0.9700
0.7946	108.8396	84.8338	73.3100	71.2354	56.5297	49.6738	0.9400	0.2527	0.9372
0.9766	54.6251	50.1818	44.9130	82.4482	75.3691	67.6416	0.8916	0.4694	0.9440
0.6382	148.0175	133.6722	121.5741	71.4176	64.5900	60.4636	0.9814	0.2264	0.9506
0.7741	142.9247	136.8673	130.7325	87.4010	82.8111	79.1892	0.9737	0.2305	0.9529
0.9571	67.6113	58.8351	46.3509	63.2179	54.8207	43.8013	0.9433	0.3786	0.9647
0.9887	61.9138	60.5316	55.9006	82.7521	81.0524	74.8721	0.9441	0.4472	0.9638
0.9890	71.5489	62.1127	59.3654	81.5693	70.9048	67.8313	0.8929	0.3464	0.9287
0.8450	123.8429	118.2108	112.5749	93.5907	89.6371	84.8084	0.9545	0.2470	0.9500
0.8528	35.3298	18.9531	10.2563	60.2670	32.4141	17.5575	0.9656	0.5793	0.9879
0.4662	14.4576	8.6805	6.7393	49.0945	30.6463	24.3930	0.9237	0.8346	0.9843
0.9717	86.0571	62.4897	43.8074	82.7496	59.9672	42.7072	0.9540	0.3242	0.9667
0.6863	145.4861	97.4660	79.3907	90.4214	61.7769	51.3129	0.8939	0.2416	0.8865
0.5979	141.5347	117.0533	101.3462	80.8797	68.0885	59.5595	0.8560	0.2277	0.8715
0.7447	161.3891	141.3041	129.5529	99.4313	87.8116	80.4412	0.9629	0.3691	0.9550
0.7228	148.6075	112.3897	95.8239	95.2818	73.5021	63.4103	0.8910	0.2846	0.8818
0.7296	157.6109	125.0001	107.7486	96.6933	77.2976	66.9889	0.9049	0.3213	0.8994
0.9992	75.9271	54.1178	43.1336	86.3626	63.3888	51.1881	0.9286	0.3690	0.9390
0.8078	156.5644	123.4509	108.7186	101.7037	83.0984	73.9341	0.9586	0.2131	0.9202
0.7991	129.8708	98.0518	86.8286	96.3875	73.7422	65.5784	0.9321	0.2685	0.9234
0.8805	114.8091	90.7150	68.0867	95.5871	76.3490	58.1405	0.9150	0.2364	0.8860
0.6211	176.0596	126.1411	102.0959	101.4805	74.6660	60.8554	0.8953	0.2410	0.8985
0.6947	165.7767	127.5641	106.7237	102.5409	79.7537	67.0895	0.9069	0.2417	0.9097
0.8023	143.5681	120.2584	108.4970	102.7628	86.8858	78.9904	0.9245	0.2400	0.9177
0.9986	68.3334	40.3405	35.6039	77.7092	47.3887	42.0566	0.8929	0.3532	0.9250
0.9004	132.9193	86.2747	78.6021	101.6504	67.5599	62.1833	0.9654	0.2366	0.9277
0.9185	133.8734	100.2270	85.5335	109.1804	82.0418	70.3721	0.9671	0.3062	0.9526
0.9317	146.6708	110.2322	95.6501	111.6144	84.7228	74.0061	0.9868	0.3000	0.9754
0.8330	149.6010	118.6643	100.8159	103.0687	83.7616	72.1547	0.9590	0.2129	0.9148
0.7711	147.3425	125.6451	104.2092	96.7604	82.8817	69.0439	0.9137	0.2807	0.9185
0.9981	71.9509	46.4723	31.4979	80.0808	52.3993	36.2997	0.9040	0.3225	0.9245
0.8799	121.9769	86.8909	62.9813	90.8877	64.9334	47.5987	0.9590	0.2730	0.9182
0.7484	156.1941	121.9520	103.5969	94.1454	77.0064	66.9813	0.9570	0.2070	0.9240
0.9996	68.1858	48.8030	40.4569	76.5739	55.8221	46.7292	0.9572	0.3626	0.9620
0.8941	146.3367	110.3490	96.8510	105.5793	80.2420	70.8017	0.9802	0.2466	0.9490
0.9674	51.7341	33.4047	26.2988	76.5889	52.0964	41.4987	0.9137	0.4681	0.9505
0.7511	159.8215	116.3187	95.1104	93.9842	70.2725	58.5447	0.9685	0.2384	0.9397
0.9602	85.3731	55.7044	42.5416	80.0936	53.3282	41.6264	0.8804	0.2702	0.9156
0.8840	124.8084	81.0463	65.6315	95.3895	64.6492	53.2997	0.9554	0.2127	0.9110
0.9702	119.5872	86.3498	76.5994	113.6724	82.4770	73.6461	0.9591	0.2811	0.9255
0.6772	160.4122	101.8730	72.6402	91.8751	61.9227	46.2144	0.9183	0.1890	0.8843
0.7579	145.6552	100.9658	83.1554	88.3189	62.9716	52.1837	0.9440	0.2121	0.9001

...

Table A.1 continues

Entropy	Mean1	Mean2	Mean3	Standard Deviation1	Standard Deviation2	Standard Deviation3	Correlation	Energy	Homogeneity
0.7054	143.2007	121.2871	95.1557	90.8397	78.0826	61.6744	0.8859	0.3557	0.9131
0.8741	133.2139	92.9900	68.4109	95.7381	67.7756	51.0334	0.9622	0.2401	0.9204
0.7209	130.5415	86.6476	63.2225	96.0349	64.6396	48.0674	0.8459	0.2724	0.8897
0.6513	142.2604	87.9863	66.8994	92.7235	58.2802	45.1683	0.8390	0.3216	0.8963
0.9956	67.0280	51.9539	37.2863	80.8563	64.5870	47.5708	0.9625	0.4073	0.9727
0.8774	153.5675	125.1716	101.5114	108.3408	89.3759	73.4480	0.9802	0.2909	0.9716
0.9063	117.7743	92.0429	75.2624	99.4865	78.4641	65.4173	0.9381	0.2494	0.9117
0.9444	119.7077	94.7824	79.6889	97.8298	78.2257	66.9606	0.9719	0.2574	0.9379
0.9999	68.1207	42.9267	30.8146	79.4017	54.3254	41.0896	0.9019	0.3442	0.9362
0.8411	143.0952	108.7854	97.4658	96.5914	74.9118	67.7770	0.9715	0.2443	0.9415
0.7233	125.1630	90.4399	76.1908	84.2475	61.9011	53.1188	0.8880	0.3151	0.9062
0.6653	153.8331	125.7984	112.1006	93.7690	79.6523	72.6163	0.8852	0.1751	0.8483
0.6294	150.3741	119.5496	96.7286	85.4430	69.1917	56.8396	0.9236	0.2704	0.9050
0.4762	183.1603	151.4162	113.8746	76.6975	66.9371	52.5294	0.8876	0.2512	0.8941
0.7926	98.5361	70.1866	52.7722	87.1427	63.9576	48.7732	0.7669	0.2480	0.8578
0.7034	146.3544	113.1603	87.5141	88.1170	69.6194	54.9875	0.9049	0.1908	0.8769
0.9397	88.8112	78.2695	66.5761	82.4985	73.4477	62.9639	0.8861	0.2855	0.9108
0.9122	135.2498	111.9808	95.9885	116.8364	97.6724	84.2353	0.9411	0.2550	0.9088
0.9600	89.7645	72.5569	59.7384	86.4471	70.4799	59.0445	0.8897	0.2700	0.8982
0.9997	74.8849	51.3988	45.9222	90.9554	64.7666	58.5633	0.9006	0.3720	0.9281
0.6708	172.0425	143.2062	124.8782	85.9488	74.4771	68.0090	0.9813	0.1909	0.9329
0.9765	58.2321	29.3339	24.9006	80.2942	43.3646	37.1767	0.9091	0.4520	0.9589
0.7105	150.2152	89.7727	74.0203	95.3501	59.1086	49.5898	0.8814	0.2779	0.9022
0.9380	103.9271	91.4170	82.0018	92.8498	82.4101	74.5953	0.9441	0.2347	0.8829
0.7934	151.0724	132.8376	119.5371	93.5388	82.9921	75.2447	0.9643	0.2073	0.9012
0.7826	136.8555	93.0809	78.9447	102.8717	71.0061	60.9093	0.8936	0.2100	0.8694
0.7262	143.1695	118.3580	99.8464	96.6938	80.3679	68.4831	0.8681	0.3220	0.9002
1.0000	84.1920	55.9649	50.1053	96.8516	65.6973	59.3590	0.9229	0.3599	0.9468
0.8881	83.4120	67.4200	55.5537	74.6760	61.8033	51.8308	0.8433	0.2603	0.9005
0.6729	168.5531	124.2457	117.1061	102.9936	78.2943	74.2376	0.8896	0.2148	0.8866

...